



HAL
open science

Minimum length scale control in a NURBS-based SIMP method

Giulio Costa, Marco Montemurro, Jérôme Pailhès

► **To cite this version:**

Giulio Costa, Marco Montemurro, Jérôme Pailhès. Minimum length scale control in a NURBS-based SIMP method. *Computer Methods in Applied Mechanics and Engineering*, 2019, 354, pp.963 - 989. 10.1016/j.cma.2019.05.026 . hal-03486991

HAL Id: hal-03486991

<https://hal.science/hal-03486991>

Submitted on 20 Dec 2021

HAL is a multi-disciplinary open access archive for the deposit and dissemination of scientific research documents, whether they are published or not. The documents may come from teaching and research institutions in France or abroad, or from public or private research centers.

L'archive ouverte pluridisciplinaire **HAL**, est destinée au dépôt et à la diffusion de documents scientifiques de niveau recherche, publiés ou non, émanant des établissements d'enseignement et de recherche français ou étrangers, des laboratoires publics ou privés.



Distributed under a Creative Commons Attribution - NonCommercial 4.0 International License

Minimum Length Scale Control in a NURBS-based SIMP Method

Giulio Costa, Marco Montemurro¹, Jérôme Pailhès

CNRS UMR 5295, I2M, Arts et Métiers ParisTech, Esplanade d'Arts et Métiers 33405 Talence, France

Abstract

Controlling the minimum size (or length scale) of the geometric features in topology optimisation analyses is of paramount importance. Particularly, the minimum length scale must always be considered according to the smallest manufacturable size. The goal of this work is to provide an intuitive methodology for controlling the minimum length scale in a NURBS density-based algorithm for topology optimisation. In this framework, the minimum length scale can be properly tailored by acting on some parameters tuning the shape of the NURBS geometric entity, i.e. degrees, number of control points and knot vectors components. The main consequence is that the proposed method does not need the introduction of an explicit optimisation constraint into the problem formulation to take into account for the minimum length scale requirement. The effectiveness of the proposed method is proven on meaningful benchmarks for both 2D and 3D applications. The results show that the minimum length scale requirement is properly met on the reassembled geometry at the end of the optimisation process.

Keywords: Topology Optimisation, NURBS hyper-surfaces, SIMP method, Minimum Length Scale

Email address: marco.montemurro@ensam.eu, marco.montemurro@u-bordeaux.fr
(Marco Montemurro)

¹Corresponding author

Preprint submitted to Computer Methods in Applied Mechanics and Engineering May 7, 2019

1. Introduction

Software for Topology Optimisation (TO) have become well-established tools in the preliminary design phase of engineering products. However, one of the most basic needs for engineers is the integration of manufacturing requirements into the TO problem formulation in order to achieve optimised as well as manufacturable solutions, see [1] and references therein. Manufacturing requirements are, in general, strongly dependent on the chosen technology: nevertheless, the minimum admissible size of structural elements constitutes a fundamental aspect, regardless the considered process.

More specifically, each technology has an intrinsic minimum achievable size. Therefore, controlling the minimum length scale of topological features in the structure to be optimised is of outstanding importance, in order to avoid obtaining an extremely performing but absolutely non-manufacturable component. One of the first methods to take into account the minimum length scale in a standard density-based strategy is described in [2] and it is implemented in the commercial software Altair OptiStruct[®] [3] for TO: the minimum length scale is imposed through a control on the slope of the pseudo-density function on the whole design domain. Such a method turns out to be computationally efficient and can replace the perimeter penalisation or the density filtering operation for mesh independence [4]. However, an important lack of consistence between the imposed minimum member size and the actually measured minimum member size at the end of the optimisation process can be remarked.

An alternative method has been proposed by Poulsen [5] and it relies on the monotonicity control of the pseudo-density function along n_d preferential directions depending on the problem dimension: $n_d = 4$ or $n_d = 13$ for 2D and 3D problems, respectively. Although this method is sound, it provides solutions with a jagged boundary; moreover, its efficiency is limited only to regular mapped meshes (the extension of the method to whatever free mesh is anything but trivial). As projection methods have been included in TO approaches, also a filter-based minimum member size control has been implemented [6]. Projection methods have been further developed by making use of the concept of “eroded”, “intermediate” and “dilated” design [7, 8]. These techniques guarantee a strict control on the minimum member size but they are computationally burdensome because they need three Finite Elements (FE) analyses (one for each density phase). The technique discussed in [7, 8] is referred as “robust formulation”, but the robustness must

be interpreted as a consistence of the length scale of the optimised configurations with respect to manufacturing imprecisions. Anyway, the minimum length scale must be *a posteriori* checked on the final (CAD reassembled) geometry. Other strategies have been developed in the framework of the very general and versatile Level Set Method (LSM) [9] applied to structural TO problems [10]. The LSM is an alternative to the density-based methods for TO: the reader is addressed to [11] for a general overview on different LSM variants and their comparison to density-based methods. Authors in [12] have developed a smart strategy to get an explicit and local control of the minimum length scale in the context of LSM, based on the mathematical concept of “structural skeleton”. Furthermore, they have extended this strategy to the Solid Isotropic Material with Penalisation (SIMP) method [13]. However, these works neglect the possible change of the skeleton in the sensitivity analysis. The drawbacks related to this aspect are discussed in [14] and a suitable solution is proposed in [15], where it is shown that a mathematically exact definition of member size does not exist. The difficulty related to the sensitivity analysis appearing in the method described in [13] has been recently overcome by authors in [16]: they combine the skeleton method with the three-phases projection method and, finally, the minimum length scale control is performed thanks to two *structural indicator functions* and two *ad hoc* constraints.

A further method for including the minimum length scale requirement in a B-Spline density-based algorithm for TO has been suggested in [17]: the proposed strategy is based on the combination of the approach presented in [18] and the three-phases projection methods [8]. However, from a theoretical viewpoint, it seems inconsistent to choose a method requiring three FE analyses in order to control a purely geometric feature.

To overcome the restrictions related to the previous approaches, a first attempt of implementation of the minimum member size constraint has been carried out in the NURBS-based SIMP method for TO developed by the present authors in [19]. In particular, the Poulsen’s minimum length scale constraint [5] was opportunely reformulated in the NURBS framework for 2D TO problems. Although results presented in [19] are consistent in terms of reassembled geometry, the method is not general enough because it is too dependent on the element size and mesh quality. In order to go beyond the first encouraging results discussed in [19], the objective of this paper is to provide an useful and meaningful formulation, which allows for handling the minimum length scale requirement in a very smart and effective way. [The main](#)

idea is to propose a method (based on a set of precise rules and relationships) able to relate the minimum member size to the characteristic parameters of the NURBS geometric entity. Particularly, the minimum length scale can be imposed by simplifying the TO problem formulation and by avoiding an explicit optimisation constraint. In the case of B-Spline entities, the minimum length scale requirement can be systematically fulfilled by tuning the number of control points and the degrees of the blending functions along each parametric direction, for both 2D and 3D TO problems. Indeed, it will be shown through numerical results that this procedure is still possible in the case of NURBS as well. However the presence of additional continuous parameters (i.e. the NURBS weights) does not allow for a rigorous justification when NURBS are used to represent the pseudo-density field. Although this approach may be too conservative in some cases, the value of the true minimum length scale (i.e. that measured on the actual optimised topology) is consistently and systematically higher than that forecast by means of the proposed procedure.

The paper is outlined as follows. The theoretical background is briefly described in section 2. The method for implicitly set a suitable minimum member size is presented and widely discussed in section 3. The effectiveness of the proposed method is proven through meaningful 2D and 3D benchmarks in section 4. Finally, section 5 ends the paper with some conclusions and perspectives.

2. Theoretical Background

2.1. The NURBS hyper-surfaces theory

The fundamentals of NURBS hyper-surfaces are briefly recalled here below. Curves and surfaces formulae, widely discussed in [20], can be easily deduced from the following relations. A NURBS hyper-surface is a polynomial-based function, defined over a *parametric space* (domain), taking values in the *NURBS space* (codomain). Therefore, if N is the dimension of the *parametric space* and M is the dimension of the *NURBS space*, a NURBS entity is defined as $\mathbf{H} : \mathbb{R}^N \rightarrow \mathbb{R}^M$. For example, one scalar parameter ($N = 1$) can describe both a plane curve ($M = 2$) and a 3D curve ($M = 3$). In the case of a surface, two scalar parameters are needed ($N = 2$) together with, of course, three physical coordinates $M = 3$. The mathematical formula of a generic NURBS hyper-surface is

$$\mathbf{H}(u_1, \dots, u_N) = \sum_{i_1=0}^{n_1} \cdots \sum_{i_N=0}^{n_N} R_{i_1, \dots, i_N}(u_1, \dots, u_N) \mathbf{P}_{i_1, \dots, i_N}, \quad (1)$$

where $R_{i_1, \dots, i_N}(u_1, \dots, u_N)$ are the piecewise rational basis functions, which are related to the standard NURBS blending functions $N_{i_k, p_k}(u_k)$, $k = 1, \dots, N$ by means of the relationship

$$R_{i_1, \dots, i_N}(u_1, \dots, u_N) = \frac{\omega_{i_1, \dots, i_N} \prod_{k=1}^N N_{i_k, p_k}(u_k)}{\sum_{j_1=0}^{n_1} \cdots \sum_{j_N=0}^{n_N} \left[\omega_{j_1, \dots, j_N} \prod_{k=1}^N N_{j_k, p_k}(u_k) \right]}. \quad (2)$$

In Eqs. (1) and (2), $\mathbf{H}(u_1, \dots, u_N)$ is a M -dimension vector-valued rational function, (u_1, \dots, u_N) are scalar dimensionless parameters defined in the interval $[0, 1]$, whilst $\mathbf{P}_{i_1, \dots, i_N}$ are the so called *control points*. The j -th control point coordinate ($X_{i_1, \dots, i_N}^{(j)}$) is stored in the array $\mathbf{X}^{(j)}$, whose dimensions are $(n_1 + 1) \times \cdots \times (n_N + 1)$. The explicit expression of control points coordinates in \mathbb{R}^M is:

$$\mathbf{P}_{i_1, \dots, i_N} = \{X_{i_1, \dots, i_N}^{(1)}, \dots, X_{i_1, \dots, i_N}^{(M)}\}, \quad (3)$$

$$\mathbf{X}^{(j)} \in \mathbb{R}^{(n_1+1) \times \cdots \times (n_N+1)}, \quad j = 1, \dots, M.$$

For NURBS surfaces, $\mathbf{P}_{i_1, i_2} = \{X_{i_1, i_2}^{(1)}, X_{i_1, i_2}^{(2)}, X_{i_1, i_2}^{(3)}\}$ and each coordinate is arranged in a matrix defined in $\mathbb{R}^{(n_1+1) \times (n_2+1)}$. The control points layout is referred as *control polygon* for NURBS curves, *control net* for surfaces and *control hyper-net* otherwise [20]. The generic control point does not actually belong to the NURBS entity but it affects the NURBS shape by means of its coordinates. A suitable scalar quantity ω_{i_1, \dots, i_N} (called weight) is related to the respective control point $\mathbf{P}_{i_1, \dots, i_N}$. The higher is the weight ω_{i_1, \dots, i_N} , the more the NURBS entity is attracted towards the control point $\mathbf{P}_{i_1, \dots, i_N}$. For each parametric direction u_k , $k = 1, \dots, N$, the NURBS blending functions are of degree p_k ; the blending function related to the parametric direction u_k can be defined in a recursive way as

$$N_{i_k, 0}(u_k) = \begin{cases} 1 & \text{if } U_{i_k}^{(k)} \leq u_k < U_{i_k+1}^{(k)}, \\ 0 & \text{otherwise,} \end{cases} \quad (4)$$

$$N_{i_k, q}(u_k) = \frac{u_k - U_{i_k}^{(k)}}{U_{i_k+q}^{(k)} - U_{i_k}^{(k)}} N_{i_k, q-1}(u_k) + \frac{U_{i_k+q+1}^{(k)} - u_k}{U_{i_k+q+1}^{(k)} - U_{i_k+1}^{(k)}} N_{i_k+1, q-1}(u_k), \quad (5)$$

$$q = 1, \dots, p_k,$$

where each constitutive blending function is defined on the knot vector

$$\mathbf{U}^{(k)} = \{\underbrace{0, \dots, 0}_{p_k+1}, U_{p_k+1}^{(k)}, \dots, U_{m_k-p_k-1}^{(k)}, \underbrace{1, \dots, 1}_{p_k+1}\}, \quad (6)$$

whose dimension is $m_k + 1$, with

$$m_k = n_k + p_k + 1. \quad (7)$$

Each knot vector $\mathbf{U}^{(k)}$ is a non-decreasing sequence of real numbers that can be interpreted as a discrete collection of values of the related dimensionless parameter u_k . The NURBS blending functions are characterised by several interesting properties: the interested reader is addressed to [20] for a deeper insight into the matter. Here, only the *local support property* is recalled since it is of paramount importance for the NURBS-based SIMP method for TO [18, 19, 21, 22, 23]:

$$R_{i_1, \dots, i_N}(u_1, \dots, u_N) \neq 0$$

$$\text{if } (u_1, \dots, u_N) \in \left[U_{i_1}^{(1)}, U_{i_1+p_1+1}^{(1)} \right] \times \dots \times \left[U_{i_N}^{(N)}, U_{i_N+p_N+1}^{(N)} \right]. \quad (8)$$

Eq. (8) means that each control point (and the respective weight) affects only a precise zone of the *parametric space*, that is precisely referred as *local support* or *influence zone*.

2.2. The Solid Isotropic Material with Penalization Method

The present work deals with both 2D and 3D TO problems, therefore the mathematical statement of the classic SIMP method is briefly described in the most general 3D case. Consider the compact Euclidean space $D \subset \mathbb{R}^3$ in a Cartesian orthogonal frame $O(x_1, x_2, x_3)$:

$$D = \{\mathbf{x} = \{x_1, x_2, x_3\}^t \in \mathbb{R}^3 : x_1 \in [0, a_1], x_2 \in [0, a_2], x_3 \in [0, a_3]\}, \quad (9)$$

where a_1 , a_2 and a_3 are three reference lengths of the domain (related to the problem at hand), defined along x_1 , x_2 and x_3 axes, respectively. Without loss of generality, the mathematical formulation is here limited, for the sake

of clarity, to the problem of minimising the compliance of a structure, subject to an equality constraint on the volume. This problem can be mathematically well-posed through several techniques, widely discussed in literature [4]. In this framework, the aim of TO is to search for the distribution of a given isotropic “heterogeneous material” (i.e. the definition of void and material zones) on the design domain D in order to minimise the virtual work of external loads applied to the structure and, meanwhile, to meet a volume equality constraint.

Let $\Omega \subseteq D$ be the *material domain*. In the SIMP approach, Ω is determined by means of a fictitious density function $\rho(\mathbf{x}) \in [0, 1]$ defined over the whole design domain D . Such a density field is related to the material distribution: $\rho(\mathbf{x}) = 0$ means absence of material, whilst $\rho(\mathbf{x}) = 1$ implies completely dense base material. The density field affects the stiffness tensor $E_{ijkl}(\mathbf{x})$, which is variable over the domain D , according to

$$E_{ijkl}(\rho(\mathbf{x})) = \rho(\mathbf{x})^\alpha E_{ijkl}^0, \quad i, j, k, l = 1, 2, 3, \quad (10)$$

where E_{ijkl}^0 is the stiffness tensor of the bulk isotropic material and $\alpha \geq 1$ a suitable parameter that aims at penalising all the meaningless densities between 0 and 1.

Considering the FE formulation of the equilibrium problem for a static analysis, the relationship among the vector of applied generalised nodal forces $\{\mathbf{f}\}$, the vector of displacements $\{\mathbf{d}\}$, and the global stiffness matrix of the structure $[\mathbf{K}]$ is

$$[\mathbf{K}] \{\mathbf{d}\} = \{\mathbf{f}\}. \quad (11)$$

Being $\{\mathbf{d}\}$ the solution of the static problem, i.e. the vector of *degrees of freedom* (DOFs) satisfying the equilibrium condition of Eq. (11), the compliance of the structure is computed as

$$c = \{\mathbf{d}\}^T [\mathbf{K}] \{\mathbf{d}\}. \quad (12)$$

The global stiffness matrix $[\mathbf{K}]$ can be expressed as

$$[\mathbf{K}] = \sum_{e=1}^{N_e} \rho_e^\alpha [\mathbf{K}_e], \quad (13)$$

where ρ_e is the fictitious density computed at the centroid of the generic element e , N_e the total number of elements, whilst $[\mathbf{K}_e]$ is the non-penalised element stiffness matrix expanded over the full set of DOFs of the structure.

The problem of minimising the compliance of a structure subject to a constraint on the overall volume can be stated as follows:

$$\begin{aligned} & \min_{\rho_e} c(\rho_e), \\ & \text{subject to:} \\ & \left\{ \begin{array}{l} [\mathbf{K}]\{\mathbf{d}\} = \{\mathbf{f}\}, \\ \frac{V(\rho_e)}{V_{ref}} = \frac{\sum_{e=1}^{N_e} \rho_e V_e}{V_{ref}} = \gamma, \\ \rho_{min} \leq \rho_e \leq 1, \quad e = 1, \dots, N_e. \end{array} \right. \end{aligned} \quad (14)$$

In Eq. (14), V_{ref} is a reference volume, $V(\rho_e)$ is the volume of the material domain Ω , while γ is the fixed volume fraction; V_e is the volume of element e and ρ_{min} represents the lower bound, imposed to the density field in order to prevent any singularity for the solution of the equilibrium problem. Of course, the design variables of the TO problem in the classic SIMP framework are the fictitious densities defined at the centroid of each element: therefore, the overall number of design variables is equal to N_e .

Problem (14) can be solved through a suitable gradient-based algorithm: to this purpose, the derivatives of both the objective and the constraint functions with respect to the elements fictitious densities must be computed and are reported here below for the sake of completeness (see [24] for more details). The partial derivative of the compliance reads

$$\frac{\partial c}{\partial \rho_e} = -\alpha \rho_e^{\alpha-1} \{\mathbf{d}\}^T [\mathbf{K}_e] \{\mathbf{d}\} = -\frac{\alpha}{\rho_e} c_e, \quad e = 1, \dots, N_e, \quad (15)$$

where $c_e = \rho_e^\alpha \{\mathbf{d}\}^T [\mathbf{K}_e] \{\mathbf{d}\}$ represents the compliance of the single mesh element e .

The partial derivative of the volume can be trivially expressed as

$$\frac{\partial V}{\partial \rho_e} = V_e, \quad e = 1, \dots, N_e. \quad (16)$$

2.3. The NURBS-based SIMP method for Topology Optimisation

The formulation of the SIMP method in the B-Spline entities framework has been firstly provided in [18] and [25]. The more general formulation in the NURBS geometric entities framework, by deeply investigating the influence of

both discrete and continuous parameters of the NURBS blending functions, is given in [19, 21, 22, 23, 26]. The main features of the NURBS-based SIMP method for TO are briefly recalled in the following because they are basic for a fruitful understanding of this paper.

In the context of the NURBS-based SIMP method, the pseudo-density field is represented through a suitable NURBS entity [19, 21, 22, 23, 26]. Therefore, a NURBS surface is used for 2D problems

$$\rho(u_1, u_2) = \sum_{i_1=0}^{n_1} \sum_{i_2=0}^{n_2} R_{i_1, i_2}(u_1, u_2) \widehat{\rho}_{i_1, i_2}, \quad (17)$$

whilst a NURBS hyper-surface is considered for 3D problems

$$\rho(u_1, u_2, u_3) = \sum_{i_1=0}^{n_1} \sum_{i_2=0}^{n_2} \sum_{i_3=0}^{n_3} R_{i_1, i_2, i_3}(u_1, u_2, u_3) \widehat{\rho}_{i_1, i_2, i_3}. \quad (18)$$

In Eqs. (17) and (18), $R_{i_1, i_2}(u_1, u_2)$ and $R_{i_1, i_2, i_3}(u_1, u_2, u_3)$ are the NURBS rational basis functions, defined according to Eq. (2). Of course, $\rho(u_1, u_2)$ in Eq. (17) represents only the third coordinate of the array \mathbf{H} of Eq. (1) in the special case $N = 2$ and $M = 3$ (the three coordinates in the *NURBS space* are the two spatial coordinates and the pseudo-density). Similarly, $\rho(u_1, u_2, u_3)$ ($N = 3$) in Eq. (18) constitutes the fourth coordinate of the array \mathbf{H} ($M = 4$). Hence, the dimensionless parameters u_1 , u_2 , and u_3 are directly related to the physical coordinates as follows:

$$u_j = \frac{x_j}{a_j}, j = 1, 2, 3. \quad (19)$$

As stated above, there are many parameters affecting the shape of NURBS entities. Among them, the NURBS control points and the related weights are identified as *design variables*. They are arranged in the arrays $\xi_1^{2D} \in \mathbb{R}^{[(n_1+1)(n_2+1)] \times 1}$ and $\xi_2^{2D} \in \mathbb{R}^{[(n_1+1)(n_2+1)] \times 1}$ for 2D problems

$$\begin{aligned} \xi_1^{2D} &= \{\widehat{\rho}_{0,0}, \dots, \widehat{\rho}_{n_1,0}, \widehat{\rho}_{0,1}, \dots, \widehat{\rho}_{n_1,1}, \dots, \widehat{\rho}_{n_1,n_2}\}, \\ \widehat{\rho}_{i_1, i_2} &\in [\widehat{\rho}_{min}, \widehat{\rho}_{max}], \quad \forall i_1 = 0, \dots, n_1, \quad \forall i_2 = 0, \dots, n_2, \end{aligned} \quad (20)$$

$$\begin{aligned} \xi_2^{2D} &= \{\omega_{0,0}, \dots, \omega_{n_1,0}, \omega_{0,1}, \dots, \omega_{n_1,1}, \dots, \omega_{n_1,n_2}\}, \\ \omega_{i_1, i_2} &\in [\omega_{min}, \omega_{max}], \quad \forall i_1 = 0, \dots, n_1, \quad \forall i_2 = 0, \dots, n_2, \end{aligned} \quad (21)$$

whilst control points and weights are collected in the arrays $\xi_1^{3D} \in \mathbb{R}^{[(n_1+1)(n_2+1)(n_3+1)] \times 1}$ and $\xi_2^{3D} \in \mathbb{R}^{[(n_1+1)(n_2+1)(n_3+1)] \times 1}$ for 3D problems

$$\begin{aligned} \xi_1^{3D} &= \{\widehat{\rho}_{0,0,0}, \dots, \widehat{\rho}_{n_1,0,0}, \widehat{\rho}_{0,1,0}, \widehat{\rho}_{n_1,1,0}, \dots, \widehat{\rho}_{n_1,n_2,0}, \dots, \widehat{\rho}_{0,0,n_3}, \dots, \widehat{\rho}_{n_1,n_2,n_3}\}, \\ \widehat{\rho}_{i_1,i_2,i_3} &\in [\widehat{\rho}_{min}, \widehat{\rho}_{max}], \quad \forall i_1 = 0, \dots, n_1, \quad \forall i_2 = 0, \dots, n_2, \quad \forall i_3 = 0, \dots, n_3, \end{aligned} \quad (22)$$

$$\begin{aligned} \xi_2^{3D} &= \{\omega_{0,0,0}, \dots, \omega_{n_1,0,0}, \omega_{0,1,0}, \omega_{n_1,1,0}, \dots, \omega_{n_1,n_2,0}, \dots, \omega_{0,0,n_3}, \dots, \omega_{n_1,n_2,n_3}\}, \\ \omega_{i_1,i_2,i_3} &\in [\omega_{min}, \omega_{max}], \quad \forall i_1 = 0, \dots, n_1, \quad \forall i_2 = 0, \dots, n_2, \quad \forall i_3 = 0, \dots, n_3. \end{aligned} \quad (23)$$

The other NURBS parameters can be identified as *design parameters*, i.e. their value is set *a priori* at the beginning of the TO analysis and is not optimised. A concise discussion on the effect of these parameters on the final optimum topology is given here below. For more details, the interested reader is addressed to [19, 23, 26].

- *The blending functions degrees*: increasing the degree implies broadening the local support size and the effect of this operation is twofold. On the one hand, a smoother boundary for the optimised topology can be got and, on the other hand, a worse convergence towards more efficient configurations is observed.
- *The control points number*: enhancing the control points number implies a smaller local support size. Thus, better performances, in terms of objective function, can be achieved and thinner topological features are allowed. Of course, this fact involves a higher number of design variables and, consequently, an increased computational burden.
- *The knot vector*: the non-trivial knot vectors components appearing in Eq. (6) have been uniformly distributed on the interval $[0, 1]$ for both 2D and 3D problems.

For the sake of synthesis, the following arrays can be defined:

$$\Xi^{(l)} = \begin{cases} \xi_l^{2D} & \text{if } N = 2, \\ \xi_l^{3D} & \text{if } N = 3, \end{cases} \quad l = 1, 2. \quad (24)$$

Moreover, the total number of control points is trivially $n_{tot} = (n_1 + 1)(n_2 + 1)$ in 2D and $n_{tot} = (n_1 + 1)(n_2 + 1)(n_3 + 1)$ in 3D. Thus, the statement of the classic TO problem of compliance minimisation subject to an equality constraint on the volume is provided through an unified formulation:

$$\begin{aligned} & \min_{\Xi^{(1)}, \Xi^{(2)}} \frac{c(\rho(\Xi^{(1)}, \Xi^{(2)}))}{c_{ref}}, \\ & \text{subject to:} \\ & \left\{ \begin{array}{l} (\sum_{e=1}^{N_e} \rho_e^\alpha [K_e])\{d\} = [K]\{d\} = \{f\}, \\ \frac{V(\rho(\Xi^{(1)}, \Xi^{(2)}))}{V_{ref}} = \frac{\sum_{e=1}^{N_e} \rho_e V_e}{V_{ref}} = \gamma, \\ \Xi_k^{(1)} \in [\hat{\rho}_{min}, \hat{\rho}_{max}], \\ \Xi_k^{(2)} \in [\omega_{min}, \omega_{max}], \\ \forall k = 1, \dots, n_{tot}. \end{array} \right. \end{aligned} \quad (25)$$

In Eq. (25), ρ_e is the generic element pseudo-density, i.e.

$$\rho_e = \begin{cases} \rho(u_1^e, u_2^e) = \rho\left(\frac{x_1^e}{a_1}, \frac{x_2^e}{a_2}\right), & \text{if } N = 2, \\ \rho(u_1^e, u_2^e, u_3^e) = \rho\left(\frac{x_1^e}{a_1}, \frac{x_2^e}{a_2}, \frac{x_3^e}{a_3}\right), & \text{if } N = 3, \end{cases} \quad (26)$$

where x_j^e is the j -th Cartesian coordinate of the element centroid. The objective function is divided by a reference compliance (c_{ref}), to obtain a dimensionless value.

The computation of the derivatives of both objective and constraint functions with respect to the design variables are needed in order to efficiently solve problem (25) through a gradient-based method. This task is achieved by exploiting the NURBS *local support property*. Particularly, the local support related to a control point $\hat{\rho}_{I_1, I_2}$ in 2D or $\hat{\rho}_{I_1, I_2, I_3}$ in 3D can be defined as

$$\begin{aligned} & S_\tau = \\ & \left\{ \begin{array}{l} S_{I_1, I_2} = [U_{I_1}^{(1)}, U_{I_1+p_1+1}^{(1)}] \times [U_{I_2}^{(2)}, U_{I_2+p_2+1}^{(2)}], \text{ if } N = 2, \\ S_{I_1, I_2, I_3} = [U_{I_1}^{(1)}, U_{I_1+p_1+1}^{(1)}] \times [U_{I_2}^{(2)}, U_{I_2+p_2+1}^{(2)}] \times [U_{I_3}^{(3)}, U_{I_3+p_3+1}^{(3)}], \text{ if } N = 3. \end{array} \right. \end{aligned} \quad (27)$$

In Eq. (27), the triplet of capital indices (I_1, I_2, I_3) identifies a specific control point or weight. For the sake of compactness, the linear index τ can be defined according to the following relationships

$$\tau = \begin{cases} I_1 + (I_2 - 1)(n_1 + 1), & \text{if } N = 2, \\ I_1 + (I_2 - 1)(n_1 + 1) + (I_3 - 1)(n_1 + 1)(n_2 + 1), & \text{if } N = 3. \end{cases} \quad (28)$$

Then, the general expressions of the derivatives of both the compliance and the volume read

$$\frac{\partial c}{\partial \Xi_\tau^{(1)}} = -\alpha \sum_{e \in S_\tau} \frac{c_e}{\rho_e} R_\tau^e, \quad (29)$$

$$\frac{\partial c}{\partial \Xi_\tau^{(2)}} = -\frac{\alpha}{\Xi_\tau^{(2)}} \sum_{e \in S_\tau} c_e \frac{\Xi_\tau^{(1)} - \rho_e}{\rho_e} R_\tau^e, \quad (30)$$

$$\frac{\partial V}{\partial \Xi_\tau^{(1)}} = \sum_{e \in S_\tau} V_e R_\tau^e, \quad (31)$$

$$\frac{\partial V}{\partial \Xi_\tau^{(2)}} = \frac{1}{\Xi_\tau^{(2)}} \sum_{e \in S_\tau} (\Xi_\tau^{(1)} - \rho_e) V_e R_\tau^e. \quad (32)$$

The scalar quantity R_τ^e , appearing in Eqs. (29) - (32) is simply a suitable NURBS rational basis function:

$$R_\tau^e = \begin{cases} R_{I_1, I_2}(u_1^e, u_2^e), & \text{if } N = 2, \\ R_{I_1, I_2, I_3}(u_1^e, u_2^e, u_3^e), & \text{if } N = 3. \end{cases} \quad (33)$$

Some consequences of outstanding importance result from the NURBS-based SIMP approach.

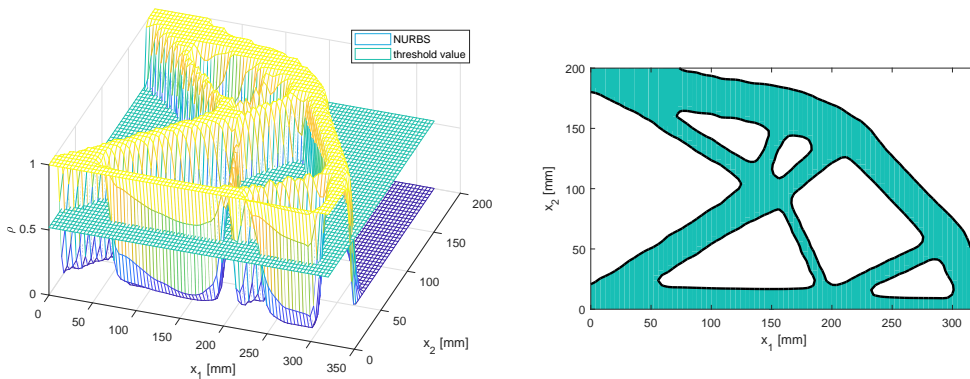
- The number of design variables is unrelated to the number of elements.
- The filtering effect deriving from the local support property: each control point (with the related weight) affects only those elements whose centroid falls in local support S_τ within the domain D . This fact is equivalent to the definition of an explicit filter in classic SIMP approaches, which is introduced in order to avoid numerical artefacts (such as the “checkerboard effect”).

For further details on the NURBS-based SIMP method, the reader is addressed to [19, 23].

3. Minimum length scale in the NURBS-based SIMP approach

3.1. Minimum length scale resulting from B-Spline entities

The minimum length scale is defined as the minimum thickness that can be identified within a structure. Consider a 2D problem: as previously specified, the pseudo-density function defines the amount of material density to be distributed in the design domain by means of control points coordinates affecting a NURBS surface. In order to retrieve the 2D optimised structure, an intersection between the surface and a suitable threshold plane is performed, as shown in Fig. 1 (see [19] for more details).



(a) NURBS surface and related threshold value.

(b) The final optimised topology of the 2D structure.

Figure 1: An example of 2D optimised topology provided by the NURBS-based SIMP method taken from [19].

Analogously, for 3D problems, the final shape can be recovered by performing the intersection between the corresponding 4D hyper-surface with the threshold density hyper-plane, as it is illustrated in Fig. 2 [23].

As the minimum length scale requirement must be satisfied on the final topology, the NURBS parameters listed in section 2 are supposed to have a strong impact on this topological feature. For the sake of clarity, only B-Spline entities are considered in a first time. In this background, some peculiar requirements need to be introduced in order to implicitly ensure a given minimum length scale, without introducing an explicit constraint into the problem formulation.

Requirement 1: The spatial coordinates of control points defining the B-Spline surface and hyper-surface are distributed according to the *Greville's abscissae* [27], i.e.

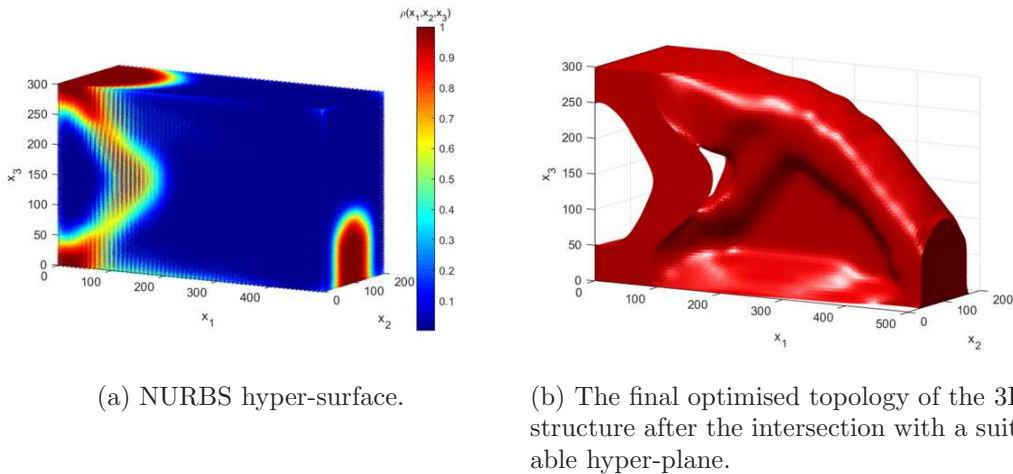


Figure 2: An example of 3D optimised topology provided by the NURBS-based SIMP method taken from [23].

$$\begin{cases} X_{I_1,*,*}^{(1)} = \frac{a_1}{p_1} \sum_{k=0}^{p_1-1} U_{I_1+k+1}^{(1)}, & I_1 = 0, \dots, n_1, \\ X_{*,I_2,*}^{(2)} = \frac{a_2}{p_2} \sum_{k=0}^{p_2-1} U_{I_2+k+1}^{(2)}, & I_2 = 0, \dots, n_2, \\ X_{*,*,I_3}^{(3)} = \frac{a_3}{p_3} \sum_{k=0}^{p_3-1} U_{I_3+k+1}^{(3)}, & I_3 = 0, \dots, n_3, \end{cases} \quad (34)$$

wherein the symbol $*$, replacing two of the three indices, aims at pointing out that the considered Greville's abscissa depends only upon the corresponding knot vector. Eq. (34) holds for 3D problems (for 2D problems, only the first two equations must be considered and index I_3 must be disregarded). Greville's abscissae guarantee that the Cartesian coordinates of the hyper-surface control points are distributed in such a way that the B-Spline evaluation at the x_j coordinate coincides exactly with x_j .

Requirement 2: the condition of minimum length scale must be [emulated](#). As far as 2D problems are concerned, the minimum member size condition is reproduced by assigning the value $\hat{\rho}_{min} = 10^{-3}$ to each control point coordinate $\hat{\rho}_{i_1, i_2}$, apart from either a column or a row of control points, which are set to $\hat{\rho}_{max} = 1$, as shown in Fig. 3a and Fig. 3c. Thanks to the *strong convex-hull property* of NURBS entities [20, 27], the pseudo-density function takes values in the interval $[10^{-3}, 1]$. The result of the intersection between the B-Spline surface and a suitable plane (representing the pseudo-density threshold value) is a strip of material phase (Fig. 3b and Fig. 3d). Of course, the thickness of this strip represents the minimum length scale, that can

be obtained along x_2 or x_1 axes if control points coordinates are set to 1 column-wise or row-wise, respectively.

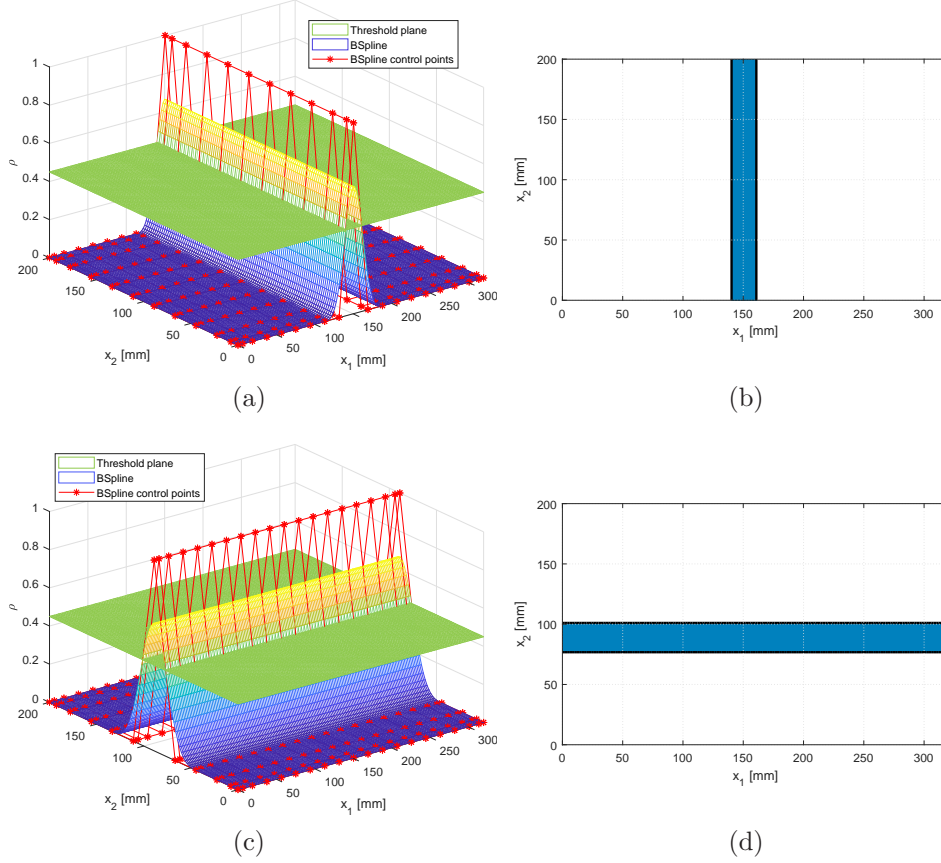


Figure 3: Emulation of 2D minimum length scale

Since control points coordinates are arranged in 3D arrays for B-Spline hyper-surfaces, a similar procedure can be repeated in 3D by setting $\hat{\rho}_{min}$ for all control point coordinates $\hat{\rho}_{i_1, i_2, i_3}$, except for those points belonging to a suitable “page” of the 3D array: e.g. the minimum member size that can be identified along the x_1 direction is detected by setting $\hat{\rho}_{I_1, i_2, i_3} = 1, \forall i_2 = 0, \dots, n_2, \forall i_3 = 0, \dots, n_3$, with an assigned I_1 . Similarly, $\hat{\rho}_{i_1, I_2, i_3} = 1, \forall i_1 = 0, \dots, n_1, \forall i_3 = 0, \dots, n_3$ and $\hat{\rho}_{i_1, i_2, I_3} = 1, \forall i_1 = 0, \dots, n_1, \forall i_2 = 0, \dots, n_2$ define the minimum length scale along x_2 and x_3 axes, respectively (see Fig. 4).

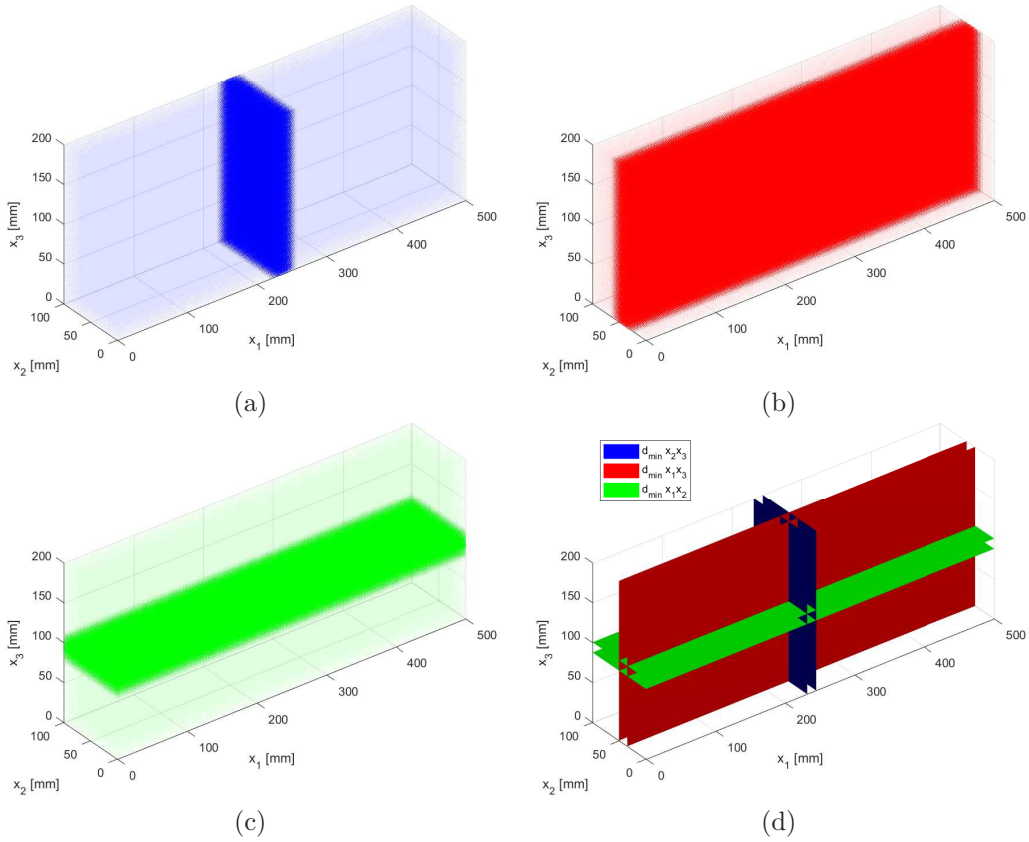


Figure 4: Emulation of 3D minimum length scale.

Requirement 3: the threshold value used for the pseudo-density field (ρ_{th}) has an impact on the minimum length scale for the problem at hand, as it can be easily inferred from Fig. 3. As observed in all the TO analyses performed in the present as well as in the previous works [19, 23], the threshold density can be set as $\rho_{th} \in [\rho_{th-LB}, \rho_{th-UB}]$, with $\rho_{th-LB} = 0.35$ and $\rho_{th-UB} = 0.6$. A deeper insight into the choice of a suitable value of ρ_{th} is provided in Section 3.2.

Requirement 4: the NURBS-based SIMP method for TO has been outlined in section 2 in its most general form. Particularly, the same methodology can be applied regardless the knot vectors components. Moreover, the Greville’s abscissae formula applies for whatever knot vector distribution. In this work, knot vectors components have been chosen uniformly spanned in the interval $[0, 1]$, unless otherwise stated, i.e.

$$\mathbf{U}^{(j)} = \left\{ \underbrace{0, \dots, 0}_{p_j+1}, \frac{1}{n_j - p_j + 1}, \dots, \frac{k_j}{n_j - p_j + 1}, \dots, \frac{n_j - p_j}{n_j - p_j + 1}, \underbrace{1, \dots, 1}_{p_j+1} \right\},$$

$$k_j = 1, \dots, n_j - p_j, \quad j = 1, 2, 3. \quad (35)$$

Thus, the distance between two non-trivial components of the knot-vector, i.e. $\Delta U^{(j)}$, is

$$\Delta U^{(j)} = \frac{1}{n_j - p_j + 1}, \quad j = 1, 2, 3. \quad (36)$$

Furthermore, it is easy to verify the following relationship among control points coordinates and the respective knot vectors components:

$$\Delta X^{(j)} = \frac{a_j}{n_j - p_j + 1} = a_j \Delta U^{(j)}, \quad j = 1, 2, 3. \quad (37)$$

The minimum length scale along a specific direction j , evaluated as detailed at *Requirement 2*, is referred as $d_{min}^{(j)}$. Considering the previous aspects, a sensitivity analysis of $d_{min}^{(j)}$ with respect to the number of control points and blending functions degree is presented in the following. For this preliminary analysis, the blending functions degrees along each parametric direction, i.e. p_j , $j = 1, 2, 3$, are kept constant and the knot-vectors components are equispaced in the range $[0, 1]$ according to Eq. (35). The logical steps of Algorithm 1 (devoted to the derivation of the minimum length scale curves) are reported here below.

Algorithm 1 Minimum length scale requirement.

- 1: Set a_j and p_j ($j = 1, 2, 3$). Set the initial value of the number of control points along each direction, i.e. n_{0j} . Initialise the slack variable $k = 1$ and set its upper bound k_{max} .
- 2: Update the control points number in each parametric direction according to

$$n_j = n_{0j} + \Delta n_j(k), \quad j = 1, 2, 3 \quad (38)$$

- 3: Evaluate the uniform knot-vector according to Eq. (35).
 - 4: Calculate Greville's abscissae according to Eq. (34).
 - 5: Determine $\Delta X^{(j)}(k)$, $j = 1, 2, 3$, according to Eq. (37).
 - 6: For 2D applications, two B-Spline surfaces denoted as $\rho_1(k)$ and $\rho_2(k)$ are created, while, for 3D problems, three hyper-surfaces $\rho_1(k)$, $\rho_2(k)$ and $\rho_3(k)$ are defined as described in *Requirement 2*.
 - 7: The minimum member size $d_{min}^j(k)$ is evaluated by performing a suitable intersection between the two B-Spline surfaces and the threshold plane in 2D or between the three B-Spline hyper-surfaces and the threshold hyper-plane in 3D. **In order to provide a general design tool, $d_{min}^j(k)$ is computed for each of the following values of threshold density: [0.35, 0.40, 0.45, 0.50, 0.55, 0.60].**
 - 8: $k = k + 1$. If $k < k_{max}$, go to point 2, otherwise go to point 9.
 - 9: The trend of d_{min}^j vs. $\Delta X^{(j)}$ is plotted.
-

The trend of d_{min}^j vs. $\Delta X^{(j)}$ is illustrated in Figs. 5 - 9 for $p_j = 3$ and for both 2D and 3D problems.

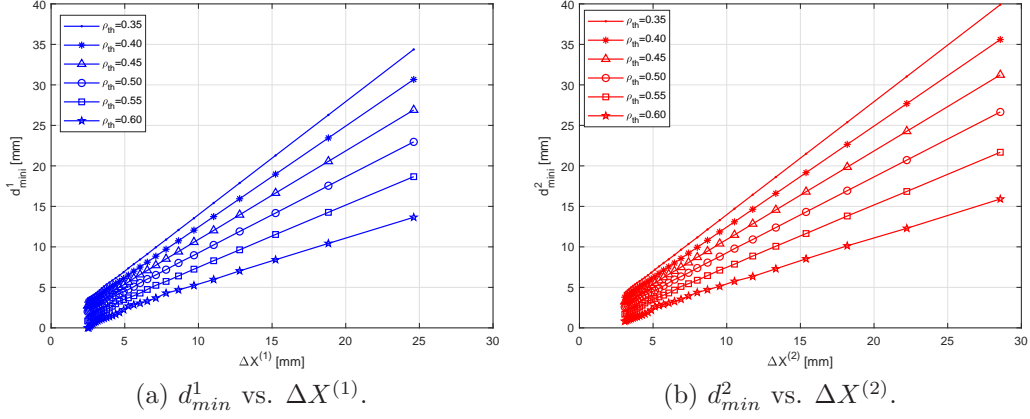


Figure 5: d_{min} trends in 2D, $p_j = 3$.

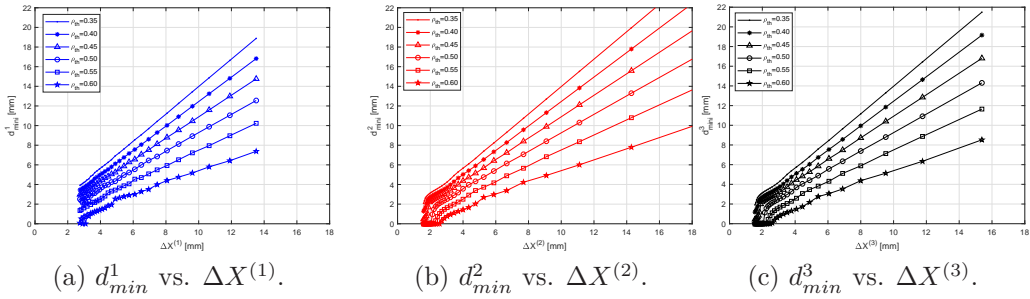


Figure 6: d_{min} trends in 3D, $p_j = 3$.

If the curves of Fig. 5, related to 2D problems, are represented on the same graph, the result is an almost perfect superposition, as shown in Fig. 7a. The same procedure is carried out for the 3D case, as shown in Fig. 6, and the result is analogous, see Fig. 7b.

As it can be deduced by the complete superposition of the curves $d_{min}^{(j)}$ vs. $\Delta X^{(j)}$ for each density threshold value, there is no need to use a specific graph for each parametric direction / physical coordinate j : thus, the superscript j can be removed and, accordingly, the minimum length scale evaluated according to *Requirement 2* (in whatever direction) is referred as d_{min} . Fig. 7 illustrates synthetic graphs on the plane d_{min} vs. ΔX for both 2D and

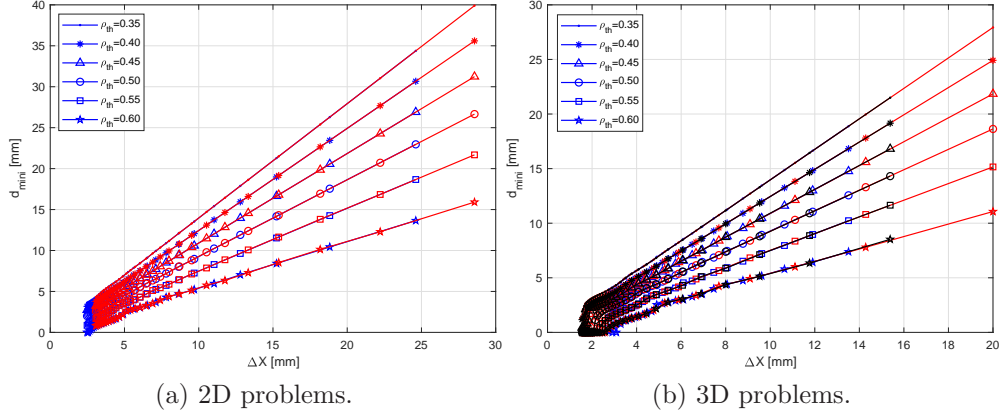


Figure 7: d_{min} vs. ΔX , $p_j = 3$.

3D problems. Of course, these graphs depend also upon the degree of the blending functions: the cases $p_j = 2$ and $p_j = 4$ are given in Figs. 8 and 9 for both 2D and 3D problems, respectively. It is highlighted that the minimum length scale corresponding to the $\rho_{th} = 0.6$ is equal to 0 when the degree of the NURBS blending functions is 4 for both 2D and 3D problems (as shown in Fig. 9). This fact simply means that there is not any intersection between the NURBS entity and the plane/hyper-plane representing the threshold density. This behaviour is due to the local support of NURBS that act as a filter zone in TO problems and it is perfectly consistent with results obtained in bibliography [19, 23].

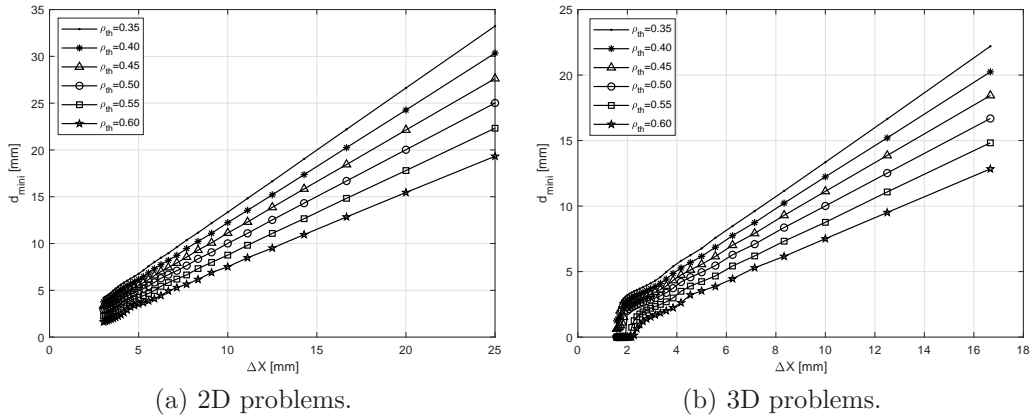


Figure 8: d_{min} vs. ΔX , $p_j = 2$.

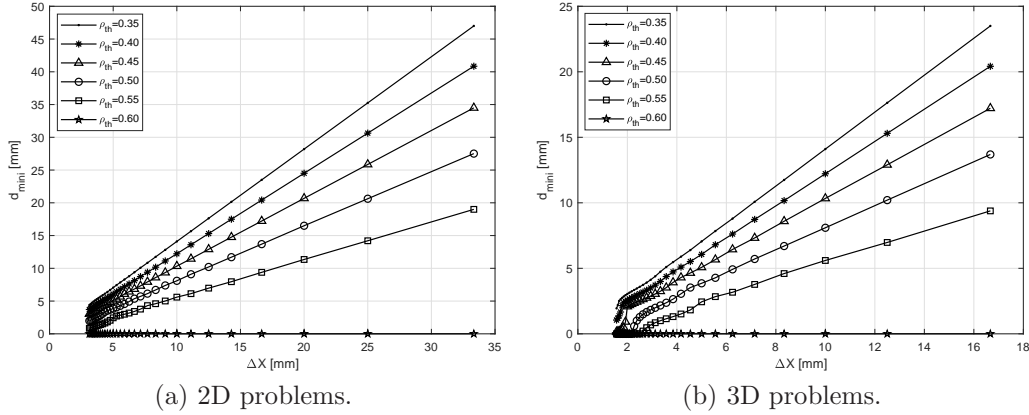


Figure 9: d_{min} vs. ΔX , $p_j = 4$.

The curves d_{min} vs. ΔX can be used as a design tool to forecast the minimum length scale for different combinations of n_j and p_j . In particular, given a certain value of d_{min} (e.g. imposed by technological requirements), the designer can choose the B-Spline degree and, through the corresponding abaci of Figs. 7-9, can select the related ΔX to be used along each physical direction x_j , $j = 1, 2, 3$ (this fact asks the designer to forecast a suitable value for the final threshold density). Through the knowledge of ΔX from Eq. (37), the designer can easily determine a suitable number of control points along each parametric direction, i.e. n_j ($j = 1, 2, 3$). Furthermore, since the knot vectors are uniform, the previous graphs can be converted in d_{min} vs. n/a curves, that is the minimum member size as a function of the control points density, as shown in Figs. 10-12. Therefore, the TO analysis is performed by setting the right number of control points: once convergence is achieved, the minimum length scale is measured on the reassembled geometry (after the cutting operation through the threshold density plane/hyperplane) and it should be verified that the minimum member size measured on the CAD model is always greater than or equal to the minimum length scale forecast by means of Figs. 7-9. This methodology does not depend on the shape of the computational domain. Whatever domain can be embedded in a rectangle in 2D and in a regular prism in 3D: the TO analysis can be carried out by simply disregarding those control points that do not affect any element of the mesh, as widely discussed in previous works [19, 23]. As the estimated minimum length scale is independent of the physical direction, the design abaci constitute very versatile tools for both academic benchmarks and industrial problems.

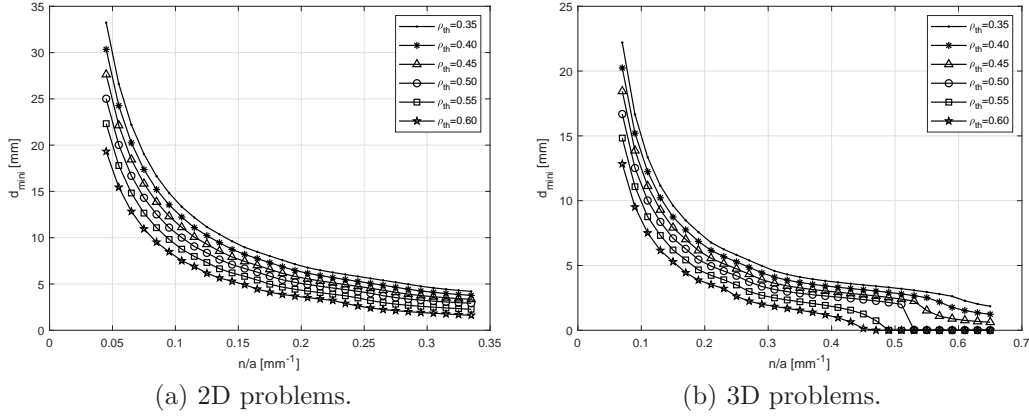


Figure 10: d_{min} vs. n/a , $p_j = 2$.

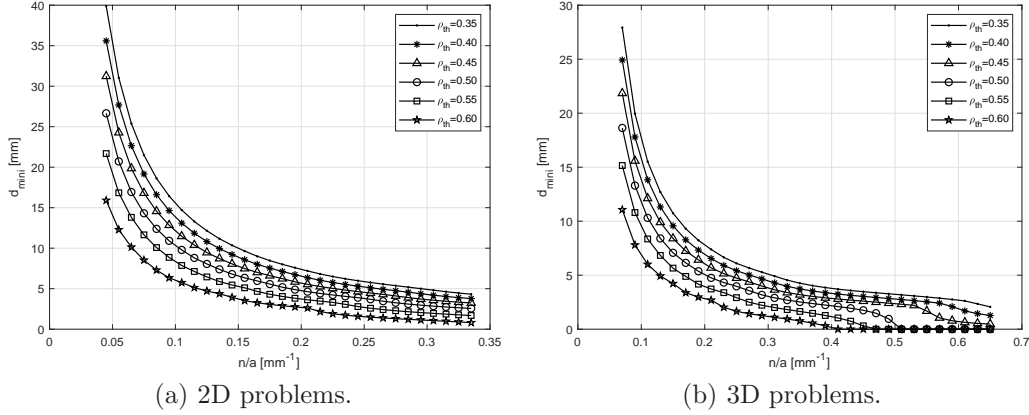


Figure 11: d_{min} vs. n/a , $p_j = 3$.

The previous procedure for determining suitable *abaci* to take into account for the minimum length scale must be slightly modified for those regions which are close to the boundary of the computational domain. This fact is perfectly logic, since the previously discussed algorithm holds for a constant $\Delta X^{(j)}$. Indeed, as control points are distributed on the reference domain by means of the Greville's abscissae formula of Eq. (34), $\Delta X^{(j)}$ is not constant and strongly varies within the regions adjacent to the boundary of the computation domain, wherein Eq. (37) should be replaced by

$$\Delta X_0^{(j)} = \frac{a_j}{p_j} \Delta U^{(j)}, j = 1, 2, 3. \quad (39)$$

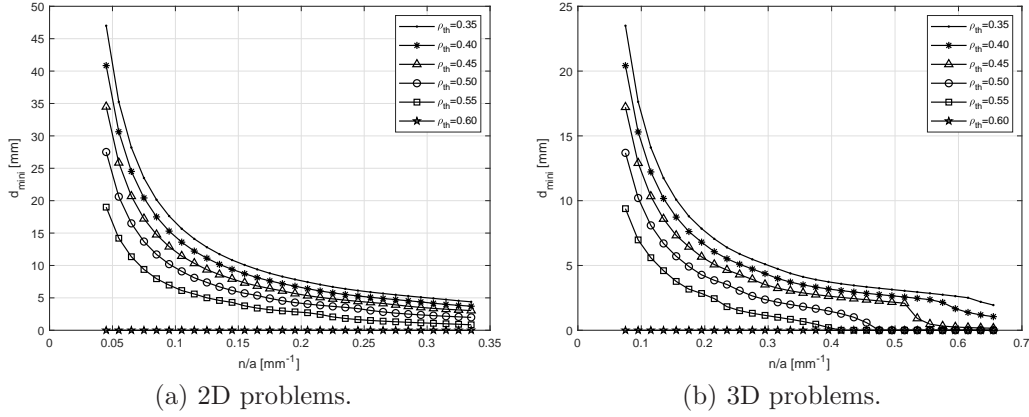


Figure 12: d_{min} vs. n/a , $p_j = 4$.

In Eq. (39), $\Delta X_0^{(j)}$ indicates the value of $\Delta X^{(j)}$ at the boundary. Therefore, the idea is to provide design *abaci* similar to those of Figs. 7-9 by using Eq. (39) at point 5 of Algorithm 1. The *abaci* related to the minimum member size near the boundary of the computation domain, which is denoted d_{min}^B , are illustrated in Figs. 13 - 15. These *abaci* show the same trend of the previous ones and they can be used as a design tool in order to forecast the minimum member size at the boundary of the design domain.

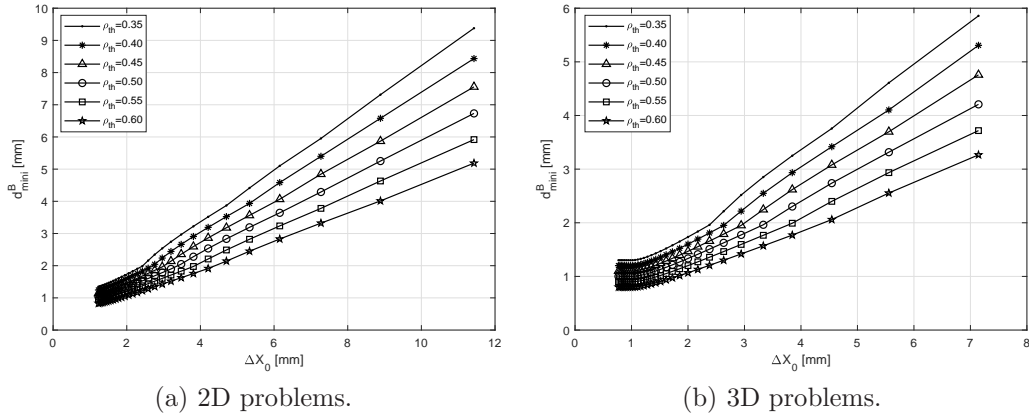


Figure 13: d_{min}^B vs. ΔX_0 , $p_j = 2$.

It is noteworthy that the minimum member size next to the computational domain boundary constitutes a special condition that deserves a particular attention. To understand this point, let consider a 2D TO problem: the

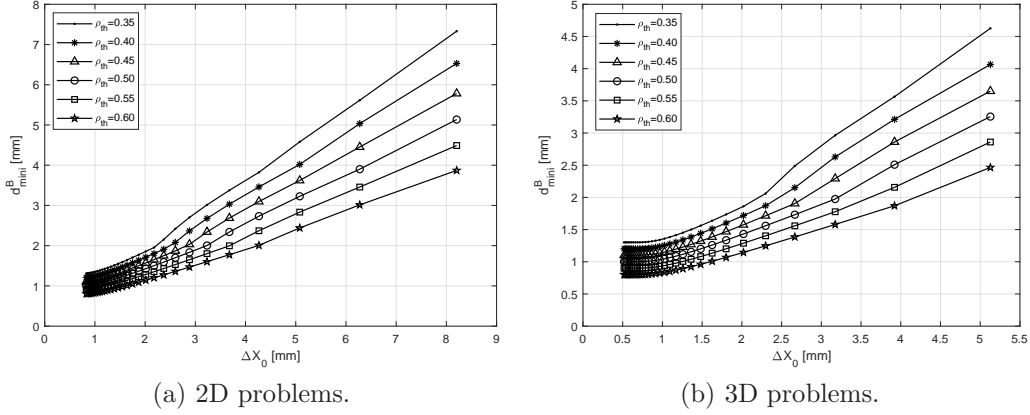


Figure 14: d_{min}^B vs. ΔX_0 , $p_j = 3$.

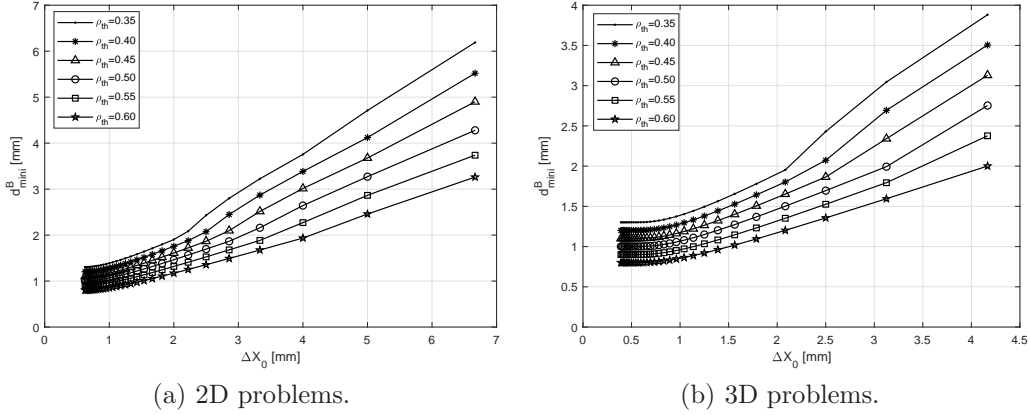


Figure 15: d_{min}^B vs. ΔX_0 , $p_j = 4$.

B-Spline degrees are set to $p_1 = p_2 = 3$ and the domain characteristic dimensions are $a_1 = 320$ mm and $a_2 = 200$ mm. Suppose that the demanded minimum member size is $d_{min} = 5$ mm. The corresponding graph of Fig. 7 is examined and it can be retrieved that $\Delta X = 5.5$ mm for an estimated threshold value $\rho_{th} = 0.5$. Accordingly, the graph of Fig. 11a provides a control points density $n/a = 0.191$. Therefore, $n_1 + 1 = 62$ and $n_2 + 1 = 39$ are enough to obtain a final design meeting the imposed minimum member size constraint. However, this control points distribution implies $\Delta X_0 = \Delta X/3 = 1.83$ mm according to Eq. (39), thus an expected minimum member size $d_{min}^B = 1.35$ mm, as it can be inferred from the graph of Fig. 14a. This result does not mean that the design will surely provide a minimum member size of 1.35

mm, but it rather warns the designer that the minimum member size could decrease up to 1.35 mm near the boundary. Under these circumstances, the designer has two choices: on the one hand, the demanded minimum member size condition can be forced on the design domain boundary, i.e. a greater ΔX_0 is chosen, and, accordingly, a smaller number of control points; on the other hand, the designer can try to run the TO computation and then analyse the resulting configuration. In any case, the method allows the designer to be aware about the effects of his choices: reducing too much the number of control points could lead to a poor description of the final topology and, consequently, to inefficient configurations. Contrariwise, launching the TO analysis with $n_1 + 1 = 62$ and $n_2 + 1 = 39$ could produce too thin features in the neighbourhood of the domain boundary, that could be unsatisfactory from a technological/mechanical viewpoint.

A smart way to overcome this dichotomy is the utilisation of a non-uniform knot vector, i.e. a knot vector which is not characterised by equally spaced components. In this case, design *abaci* similar to those of Figs. 7 - 9 can be provided. However these graphs are not reported here for sake of brevity. Rather, the beneficial effect of the use of a non-uniform knot vector on the final optimised topology and on the related minimum length scale is directly illustrated on a meaningful benchmark in section 4.

3.2. Some remarks about the proposed approach

The approach making use of the previous *abaci* presents different aspects of outstanding importance.

The method is simple and intuitive to the designer and does not need the introduction of a further constraint in the TO problem formulation. This fact is of paramount importance because constraints involving the minimum member size are often burdensome from a computational viewpoint. Furthermore, these constraints are not met on the reassembled geometry at the end of the optimisation process in the most of the cases. Contrariwise, the proposed approach allows for setting a pertinent combination of number of control points and degrees of the NURBS blending functions that automatically satisfy the imposed minimum member size. [The aim of the design abaci is to forecast \$d_{min}\$ on the reassembled geometry without any explicit optimisation constraint. This method has been conceived in order to promote the consistence between estimated and actual minimum length scale. As a side effect, the methodology could under-estimate the minimum length scale for](#)

some combinations of NURBS degrees and number of control points: therefore, the actual minimum length scale measured on final configurations could be higher than the estimated one. A thoughtful discussion on this aspect is provided in Section 4.

Even if the advantages of the NURBS-based SIMP approach have been already shown in previous works [18, 19, 23, 25], the choice of the NURBS discrete parameters (i.e. the number of control points and/or the degree) was not unique and it was left to the designer experience. By means of the abaci of Figs. 7-9, it is possible to choose a suitable number of control points by setting the desired minimum member size.

Nevertheless, the proposed method is not free of drawbacks. There are two most evident issues to be discussed. Firstly, the designer must arbitrarily set the degree of the blending functions and, *a priori*, he should try several degrees in order to understand the influence of this parameters on the final optimum topology. Secondly, the designer is obliged to set a threshold density. However, the actual value of this quantity is provided at the end of the optimisation in order to meet the imposed constraints [19, 23]; this means that ρ_{th} is unknown before performing the TO analysis. Anyway, these are only minor issues that can be easily overcome.

The range of degrees to be used for the TO analysis is limited because, as widely explained in [19, 23], high degrees hamper the correct convergence of the algorithm towards an efficient solution, especially when the number of control points is low. Therefore, there is no interest in using high degrees and the designer can try just the values $p_j = 2, 3, 4$.

Accounting for the gained experience on solving TO problems through the NURBS-based SIMP approach, a likely value for the threshold density is 0.5 and 0.45 for 2D and 3D applications, respectively. Then, if the problem at hand presents particular constraints, which could lead to a poor convergence rate, the previous values can be reduced. If the designer is uncertain among two values for ρ_{th} , the highest value should be set in order to make the most conservative choice.

3.3. The effects of the NURBS weights on the minimum length scale

Including the NURBS weights among the design variables leads to some advantages. As discussed in [19, 23], better performances can be achieved when weights and control points are optimised at the same time and final geometries exhibit a smoother boundary. However, their use should be carefully assessed because choosing a NURBS rather than a B-Spline implies

doubling the number of design variables if the same number of control points is used.

The minimum member size should be forecast in the case of NURBS as well. The main difficulty raised by considering the weights as design variables consists of the lack of a simple relationship between physical coordinates and the respective knot vector. In other words, the Greville’s abscissae formula in the form of Eq. (34) does no longer apply, so it is not possible to easily calculate the physical coordinates x_j , $j = 1, 2, 3$ of the control points within the design domain. Moreover, it should be remarked that weights are now design variables and that their value is not *a priori* known. Since the previously depicted method seemed to be sound enough for B-Splines entities, it is sought to exploit the methodology also in the case of NURBS entities.

To this purpose, the simple benchmark of Fig. 1 has been considered: it is the solution of the TO problem (25) for a 2D aluminium plate clamped on the left side and subject to a shear load applied to the right-bottom corner taken from [19]. The NURBS discrete parameters were set as $n_1 = 47$, $n_2 = 29$ and $p_1 = p_2 = 3$. The idea is to observe the behaviour of the pseudo-density and weights along horizontal lines related to specific control points rows. Particularly, it is sought to identify some minimum length scale condition, corresponding, for instance, to the thin topological element appearing in the middle-bottom zone of the domain represented in Fig. 1b. In order to have a clearer picture of the situation, Fig. 16 reports the optimised topology observed in Fig. 1b together with the trends of pseudo-density and weights at control points evaluated along the green lines.

Graphs of Fig. 16 confirm that the d_{min} condition occurs when a single control point takes the value 1 whilst its neighbours take the value 0. In this particular condition, the attention is focused on the trend of the corresponding weights: the weight related to the peak control point is always greater than 1, whilst the weights related to the two closest control points at the two sides of the peak are lower than 1. In practice, when the minimum length scale condition is emulated, the pseudo-density field is more attracted towards the material phase when it is represented by means of a NURBS entity rather than a B-Spline one. Thus, the most critical condition (i.e. the lowest value of member size) is obtained with B-Spline surfaces and not with NURBS surfaces. The natural conclusion of this study is that the design graphs of section 3.1 can be used for B-Spline and NURBS entities as well, since in any case they will constitute a conservative estimation of the minimum length scale.

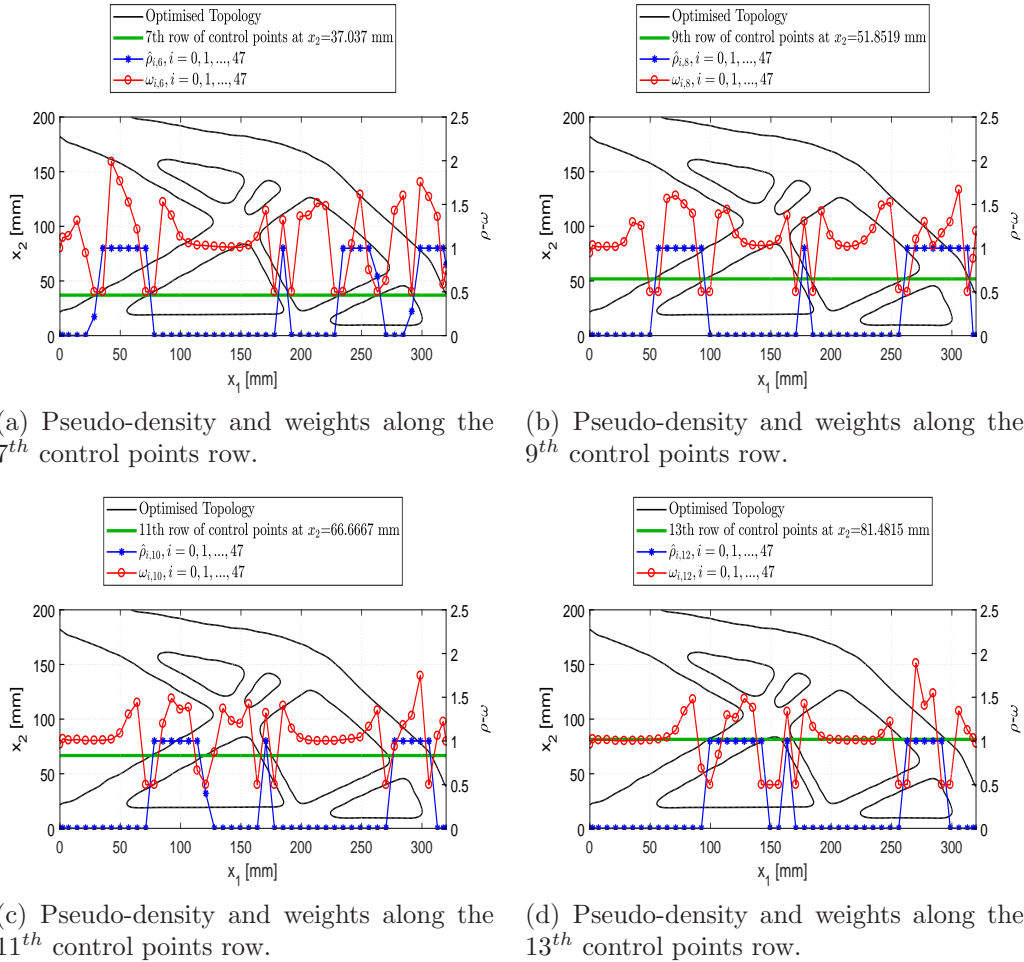


Figure 16: Weights and Control Points trends for a NURBS solution.

Of course, when NURBS entities are considered, the aforementioned abaci should be used with caution. The use of the design graphs, that is sound for B-Spline entities, can be only partially justified for NURBS entities. Indeed, the graphs of section 3.1 are referred to ΔX and n/a . In the case of NURBS entities, these quantities must be interpreted as average quantities, since it is not possible to locate control points according to the Greville's abscissae formula.

Finally, even if the validity of the proposed method cannot be rigorously justified in the case of NURBS entities, its effectiveness is empirically shown

on some meaningful benchmarks in section 4.

4. Results

4.1. Minimum length scale in 2D

The effectiveness of the abaci presented in section 3 is proven here in the case of 2D problems through the simple benchmark of Fig. 17 (refer to related caption for details about the geometry and the FE analysis). The

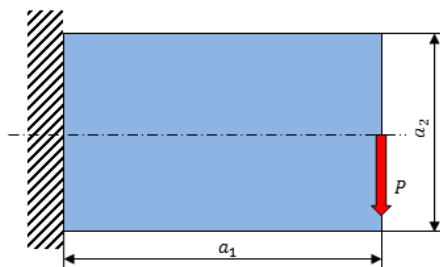


Figure 17: 2D benchmark - Geometric parameters: $a_1 = 320$ mm, $a_2 = 200$ mm, thickness $t = 2$ mm - Material parameters: $E = 72000$ MPa, $\nu = 0.33$ - Mesh: 96×60 PLANE182 elements (plane stress formulation) - Load: $P = 1000$ N.

TO problem is formulated according to Eq. (25), where $V_{ref} = a_1 a_2 t$ and $\gamma = 0.4$. Furthermore, a symmetry condition is imposed with respect to the plane $x_2 = a_2/2$. The TO problem is solved by means of the NURBS-based SIMP method described in Section 2.3. Details about the architecture of the corresponding algorithm for TO, called SANTO (SIMP And NURBS for Topology Optimisation) and developed at the I2M Laboratory, can be found in [23, 26]. When the solution is achieved, the result is exported in Initial Graphics Exchange Specification (IGES) format and the 2D solution is retrieved by means of the threshold operations described in [19, 21]. This operation is performed in the CAD environment of CATIA[®], as shown in Fig. 18a. Once the 2D structure is obtained, the actual minimum thickness of structural elements is identified and measured. The concept of minimum length scale is pretty clear but a mathematically exact definition does not exist. Accordingly, the measured minimum length scale can be conventionally defined as the diameter of the smallest circle inscribed within the structure such that a slight increment of its diameter would exceed the boundary of the structure itself (an example is given in Fig. 18b).

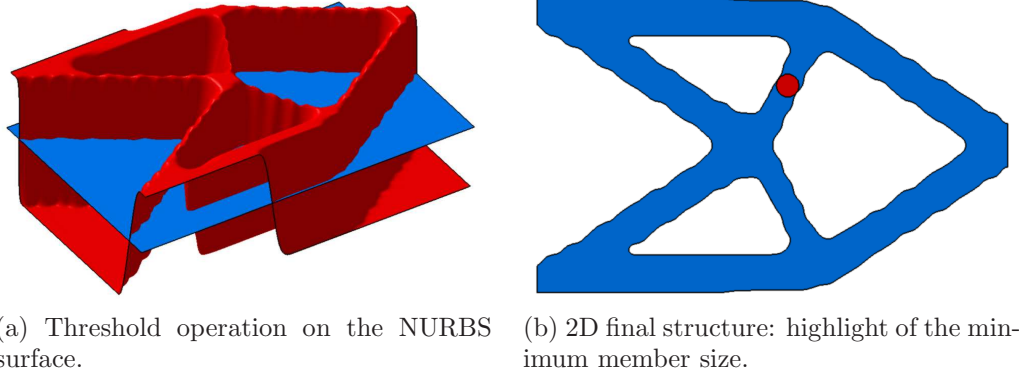


Figure 18: Procedure to measure the actual minimum member size.

The method presented in section 3 is tested by comparing the minimum length scale predicted by graphs of Figs. 10-12 and Figs. 13-15 to the measured minimum member size on the actual reassembled structure. To this purpose, the benchmark problem has been solved by making use of both B-Spline and NURBS surfaces (polynomials degrees $p_j = 3$, $j = 1, 2, 3$) and the TO analysis has been repeated several times in order to change the number of control points. This campaign of results has been carried out by means of uniform knot vectors.

Solutions are shown in Fig. 19 and numeric results are collected in Tables 1 and 2, wherein the compliance is divided by a reference quantity $c_{ref} = 2625$ Nmm, that is the compliance of the structure with an uniform initial density $\rho(u_1, u_2) = \gamma$. The measured minimum length scale is referred as d_{min}^M , whilst the forecast value of the minimum length scale is referred as d_{min} on the internal zones and d_{min}^B on the boundary of the design domain, respectively. The two values d_{min} and d_{min}^B are evaluated for an estimated threshold value of the density $\rho_{th} = 0.5$.

In the following Tables, the (*B*) symbol appears next to the values of d_{min}^M when the minimum member size is measured in the neighbourhood of the boundary; otherwise, the critical zone, wherein d_{min}^M is measured, occurs within the design domain.

As it can be retained from Tables 1 and 2, the minimum length scale is correctly forecast for both B-Spline and NURBS solutions. The previous statement must be interpreted in the sense that the minimum length scale that is forecast through the proposed methodology is always lower than

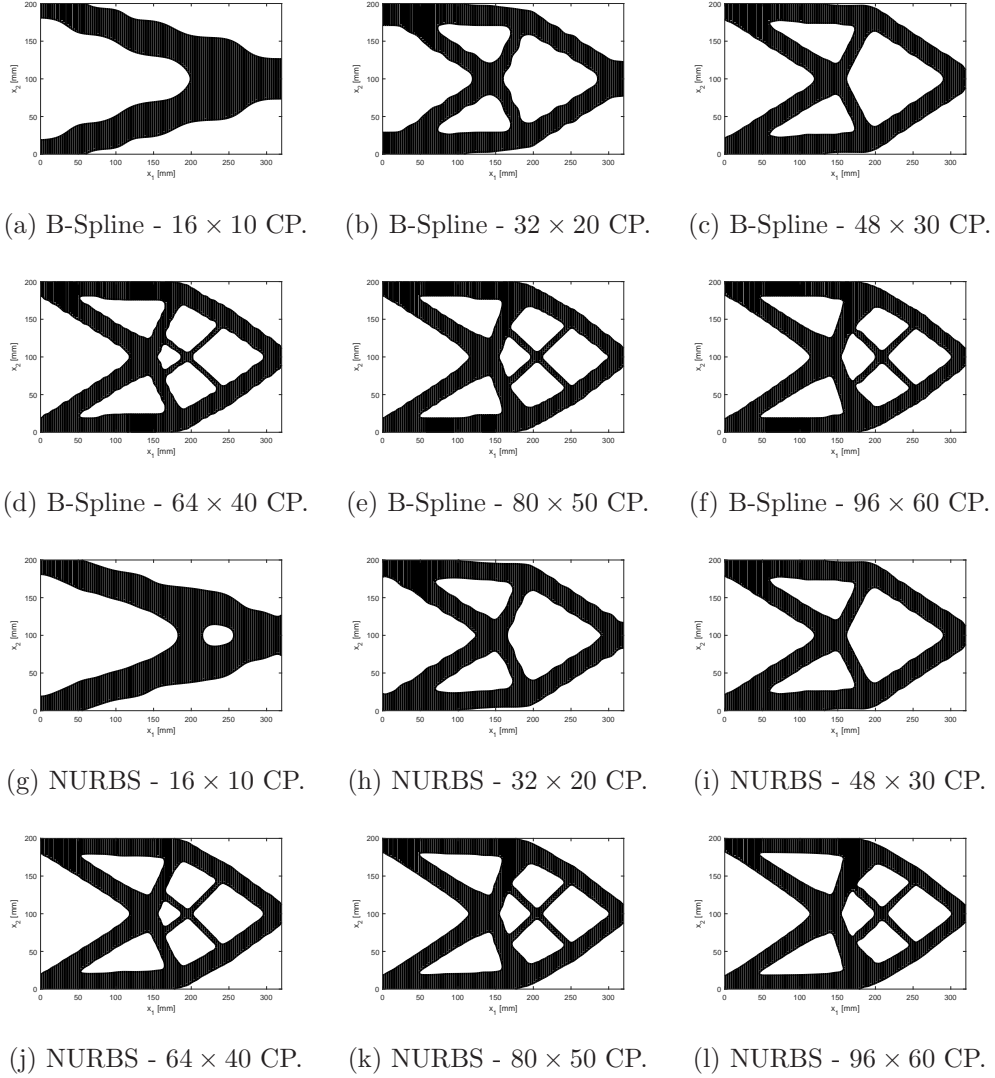


Figure 19: 2D solutions - minimum length scale, $p_j = 3$.

the actual minimum length scale that is measured on the CAD-reassembled geometry. In this sense the method is conservative.

4.2. Minimum length scale in 3D

Because of the complexity of 3D topologies, the minimum length scale condition is checked in a different way with respect to the case of 2D struc-

n_{tot}	c/c_{ref} [Nmm]	d_{min}^M [mm]	d_{min} [mm]	d_{min}^B [mm]
16×10	0.263	19.705 (B)	26.650	5.14
32×20	0.178	16.340	12.010	2.34
48×30	0.151	16.170	6.765	1.59
64×40	0.146	5.173	4.937	1.32
80×50	0.144	6.470	3.575	1.16
96×60	0.145	4.960	2.910	1.08

Table 1: Minimum length scale for 2D B-Spline solutions

n_{tot}	c/c_{ref} [Nmm]	d_{min}^M [mm]	d_{min} [mm]	d_{min}^B [mm]
16×10	0.210	18.905 (B)	26.650	5.14
32×20	0.154	14.470	12.010	2.34
48×30	0.142	17.159	6.765	1.59
64×40	0.142	6.586	4.937	1.32
80×50	0.143	6.946	3.575	1.16
96×60	0.145	7.301	2.910	1.08

Table 2: Minimum length scale for 2D NURBS solutions

tures. The problem of Eq. (25) is solved for the benchmark of Fig. 20. Two symmetry conditions, with respect to the planes $x_2 = a_2/2$ and $x_3 = a_3/2$, are added. Solutions are provided in the following for different control points numbers and by setting the B-Spline/NURBS hyper-surfaces degrees equal to 3.

For 3D problems, the optimised configurations can be handled, at the end of the optimisation process, *via* suitable [Standard Tessellation Language \(STL\)](#) files. The graphs of section 3 can be used in order to forecast the minimum member size within the domain and on its boundary. The STL file collects the n_{TR} triangles composing the boundary of the optimised volume, thus the local outward normal vector \mathbf{n} can be identified on each boundary surface. This information can be exploited to measure the actual minimum member size at the end of the optimisation, in order to check the effectiveness and the robustness of the approach based on the abaci illustrated in section 3.1.

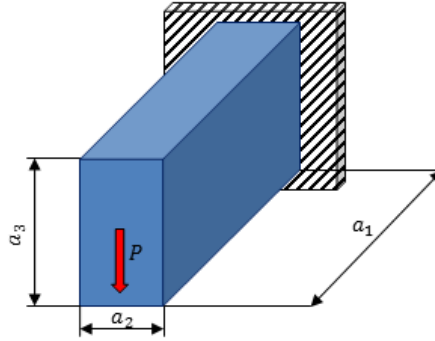


Figure 20: 3D benchmark - Geometric parameters: $a_1 = 400$ mm, $a_2 = 100$ mm, $a_3 = 200$ mm - Material parameters: $E = 72000$ MPa, $\nu = 0.33$ - Mesh: $64 \times 16 \times 32$ SOLID185 elements - Load: $P = 2000$ N.

It is noteworthy that the boundary of the 3D continuum is retrieved from the knowledge of the iso-surface $\rho = \rho_{th}$ of the fictitious density field. Considering the normal vector, the fourth coordinate of the NURBS hypersurface (which describes the pseudo-density field) takes values $\rho < \rho_{th}$ (no material phase) along the outward direction and $\rho > \rho_{th}$ along the inward direction (material phase). Therefore, the idea is to move from the iso-surface towards the material phase at least for a distance equal to the minimum member size and to check if the opposite side of the boundary is still in the material phase. The main steps realising such operations are described in Algorithm 2, which is carried out in Matlab environment.

Algorithm 2 Minimum length scale check for 3D problems.

- 1: Retrieve the total number of triangles n_{TR} from the STL file. Two counters are set $n_F = 0$ (number of feasible triangles) and $n_{UF} = 0$ (number of infeasible triangles). Set $j = 0$.
 - 2: $j = j + 1$.
 - 3: Determine the Cartesian coordinates of the center of gravity of the j -th triangle, i.e. \mathbf{OG}_j .
 - 4: If the topology boundary is inside the computation domain, move along the local inward direction according to $\mathbf{OG}'_j = \mathbf{OG}_j - d_{min} \mathbf{n}$; if the topology boundary is located on the boundary of the computation domain move along the local inward direction according to $\mathbf{OG}'_j = \mathbf{OG}_j - d_{min}^B \mathbf{n}$
 - 5: The B-Spline/NURBS is evaluated in \mathbf{OG}'_j : if $\rho_{\mathbf{OG}'_j} > \rho_{th}$, $n_F = n_F + 1$; otherwise, if $\rho_{\mathbf{OG}'_j} < \rho_{th}$, $n_{UF} = n_{UF} + 1$.
 - 6: If $j < n_{TR}$ go to point 2, else go to point 7.
 - 7: Evaluate the fraction of triangles satisfying the minimum length scale, i.e. $f_F = n_F/n_{TR}$. The fraction of triangles violating such a constraints is denoted as $f_{UF} = 1 - f_F$
-

Numerical results are collected in Tables 3 and 4: the objective function value is highlighted together with the forecast minimum length scale within the domain d_{min} and on the boundary d_{min}^B for each solution. The fractions f_F and f_F^B of “feasible” triangles are reported as well.

n_{tot}	c/c_{ref} [Nmm]	d_{min} [mm]	d_{min}^B [mm]	f_F	f_F^B
$24 \times 6 \times 12$	0.0873	15.000	5.000	0.978	0.958
$30 \times 12 \times 18$	0.0700	10.295	2.356	0.936	0.974
$36 \times 18 \times 24$	0.0620	6.136	1.522	0.982	0.999

Table 3: Minimum length scale for 3D B-Spline solutions

The topologies corresponding to the configurations appearing in Tables 3 and 4 are shown in Figs. 21-23 for B-Spline solutions and in Figs. 24-26 for NURBS solutions. In particular, the red boundary highlights the domain regions where the minimum length scale is correctly forecast, whilst the blue boundary is constituted of “infeasible” triangles, i.e. those zones characterised by a thickness smaller than that forecast by means of the abaci presented in section 3.

n_{tot}	c/c_{ref} [Nmm]	d_{min} [mm]	d_{min}^B [mm]	f_F	f_F^B
$24 \times 6 \times 12$	0.0706	15.000	5.000	1.000	0.880
$30 \times 12 \times 18$	0.0653	10.295	2.356	0.924	0.971
$36 \times 18 \times 24$	0.0608	6.136	1.522	1.000	0.998

Table 4: Minimum length scale for 3D NURBS solutions

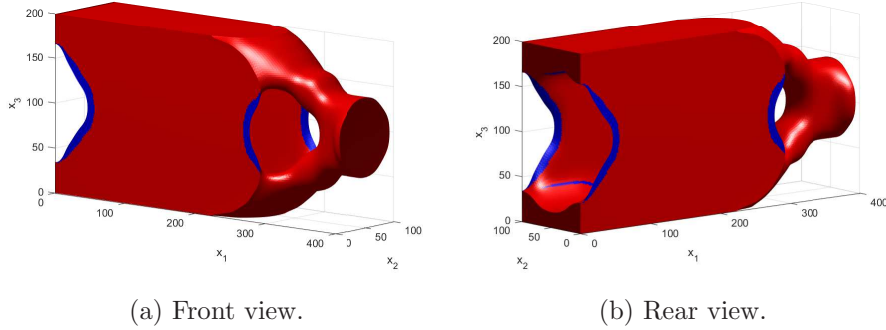


Figure 21: Highlight of the minimum length scale in 3D, B-Spline solution, $p_j = 3$, $24 \times 6 \times 12$ control points.

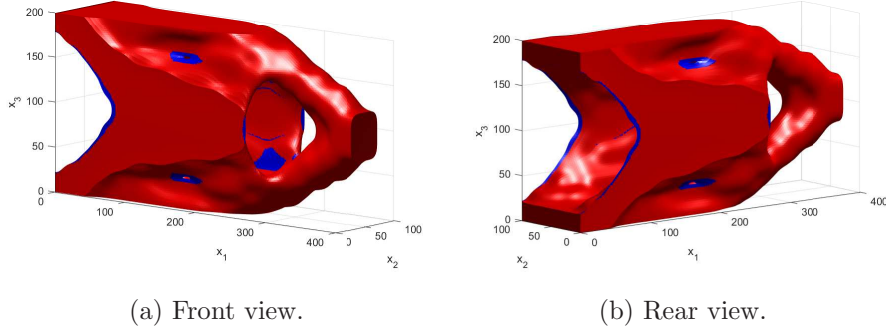


Figure 22: Highlight of the minimum length scale in 3D, B-Spline solution, $p_j = 3$, $30 \times 12 \times 18$ control points.

Results clearly show that the minimum length scale is correctly forecast in a wide zone of the domain. The minimum member size is smaller than the predicted value only in very circumscribed regions. The fractions of Tables 3 and 4 are not exactly 1 because of several reasons. Firstly, the estimation of

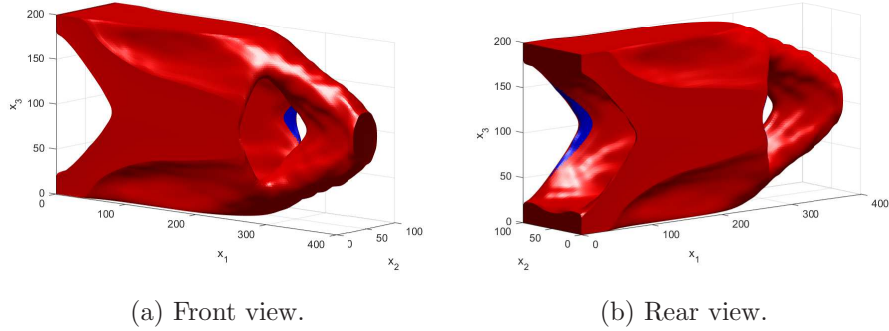


Figure 23: Highlight of the minimum length scale in 3D, B-Spline solution, $p_j = 3$, $36 \times 18 \times 24$ control points.

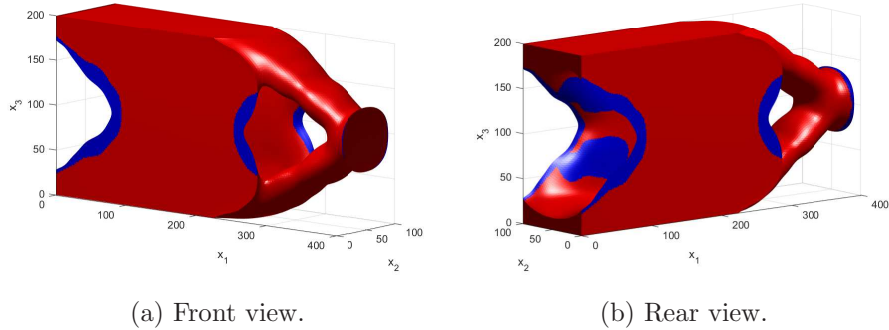


Figure 24: Highlight of the minimum length scale in 3D, NURBS solution, $p_j = 3$, $24 \times 6 \times 12$ control points.

the minimum member size is based on the assumptions described in section 3, which could be not met in whatever circumstances. Secondly, while the method seems quite intuitive in 2D, its extrapolation in 3D is not immediate. In particular, for 3D problems the evaluation of the pseudo-density threshold value is not unique and a trial-and-error approach is often required (at the end of the optimisation process) before achieving a good compromise in terms of performances and minimum length scale requirement.

However, it is noteworthy that the methodology based on the use of abaci presented in section 3 is both simple and reliable enough to be used in the NURBS-based SIMP algorithm. As far as the computational cost is concerned, it varies depending on the problem at hand. The computational

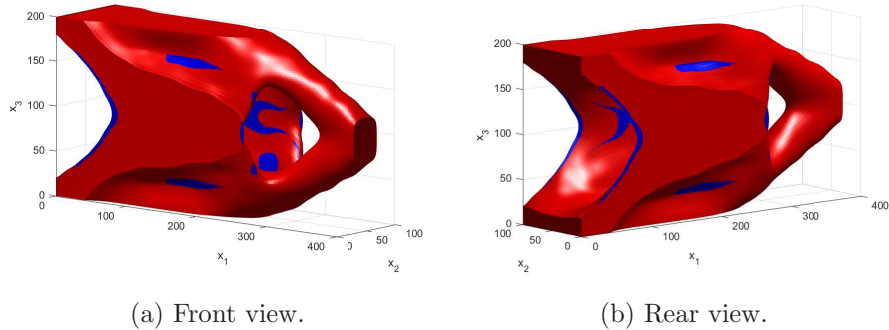


Figure 25: Highlight of the minimum length scale in 3D, NURBS solution, $p_j = 3$, $30 \times 12 \times 18$ control points.

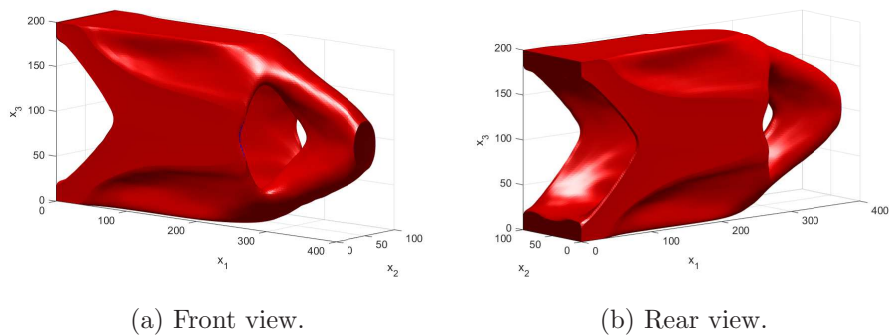


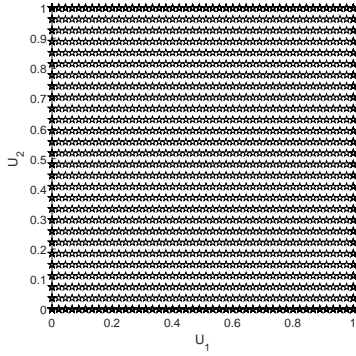
Figure 26: Highlight of the minimum length scale in 3D, NURBS solution, $p_j = 3$, $36 \times 18 \times 24$ control points.

cost is, of course, mainly related to the FE analysis and to the number of iterations needed to satisfy one of the convergence criteria at the basis of the active-set algorithm of the *fmincon* tool. In particular, all the optimisation calculations have been performed by using two cores of a work-station with an Intel *Xeon E5-2697v2* processor (2.703.50 GHz). The simulation time varies from ten minutes for the solution illustrated in Fig. 19 (100 iterations) to 20 hours (400 iterations) for the solution of Fig. 26.

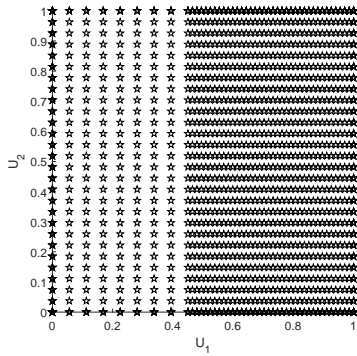
4.3. The effects of a non-uniform knot vector on the minimum length scale

Since only uniform knot vectors have been considered until now, it seems interesting to investigate the influence of a non-uniform knot vector on the

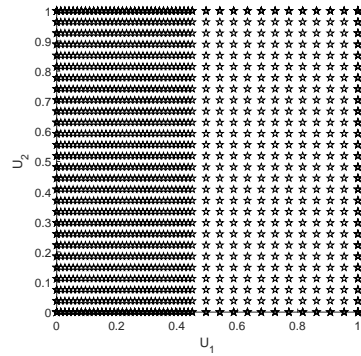
optimised topology. At the same time, the robustness of the method for predicting the minimum length scale is tested. Here, only 2D TO problems are considered, but the extension of results to the 3D case is straightforward. Let us consider the 2D benchmark of section 4.1, and, in particular, the solution corresponding to $(n_1 + 1) \times (n_2 + 1) = 48 \times 30$ (Figs. 19c and 19i illustrate the B-Spline and the NURBS solutions, respectively). Let now focus on the knot vectors distributions: in cases of Figs. 19c and 19i, the net constituted by the knot vectors components is represented in Fig. 27a. Of course, there is a strict analogy between the knot vectors components distribution in the parametric domain and the control points distribution in the physical space. Two non-uniform distribution of the knot-vector components are considered for this example: they are shown in in Figs. 27b and 27c.



(a) Uniform distribution.



(b) Clumping 1.



(c) Clumping 2.

Figure 27: Knot vectors distributions.

The same optimisation problem is run for the 2D cantilever plate by applying these two different knot vectors and results are shown in Fig. 28 for B-Spline surfaces and in Fig. 29 for NURBS ones.

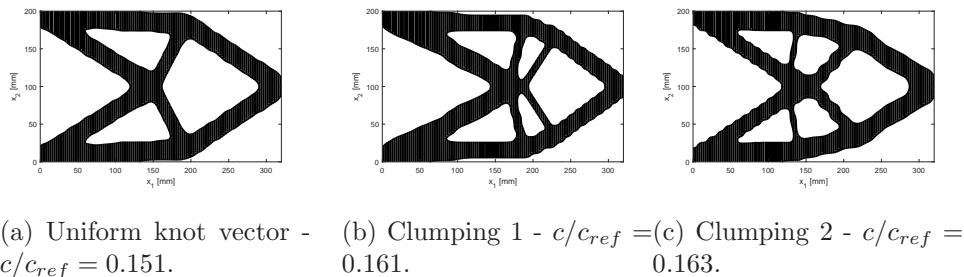


Figure 28: B-Spline solutions with different knot vector distributions.

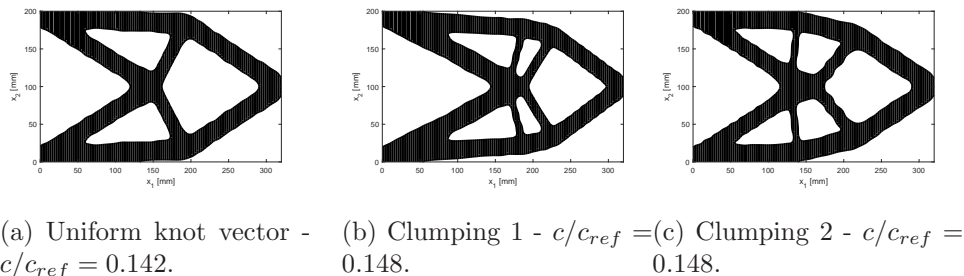


Figure 29: NURBS solutions with different knot vector distributions.

The results of Figs. 28 and 29 highlight one strong potential of the NURBS-based algorithm for TO: for the same mesh, the same number of control points and the same polynomials degrees, the user can opportunely set the knot vector components (which constitute further degrees of freedom of the proposed method) to obtain different topologies. It is interesting to check that the minimum member size forecast by means of the graphs of section 3 is always conservative (the estimated threshold value is $\rho_{th} = 0.5$). In fact, if the first knot vector clumping is considered, the most critical value $\Delta X = 4.756$ mm is obtained along the X_1 direction on the right side of the domain: the corresponding minimum member size, forecast by using the graph of Fig. 7, is $d_{min} = 4.314$ mm. The effective (measured) minimum

member size is $d_{min}^M = 7.7$ mm for the B-Spline solution (Fig. 28b) and $d_{min}^M = 7.6$ mm for the NURBS solution (Fig. 28c). As far as the second knot vector clumping is considered, the critical value $\Delta X = 4.367$ mm is obtained along the X_1 direction on the left side of the domain. In this case, $d_{min} = 3.986$ mm and $d_{min}^M = 5.1$ mm for the B-Spline solution (Fig. 29b) while $d_{min}^M = 7.0$ mm for the NURBS solution (Fig. 29c). Therefore, these results put in evidence that, when the number of control points is kept constant, the designer can distribute the knot vectors components in order to have different dimensions of topological features on specified domain zones. Moreover, the generality of the method of section 3 is proven, since the ΔX must be interpreted as a local information, regardless the considered knot vector components distribution.

5. Conclusions

In this work, an innovative method to effectively handle the minimum member size in TO problems has been presented in the framework of the NURBS-based SIMP approach.

The most relevant contribution of the proposed strategy relies on the fact that, thanks to NURBS entities properties, it is possible to forecast the minimum length scale by simply choosing the NURBS discrete parameters (number of control points and degrees) and some of their continuous parameters, like knot vectors components, by making use of very general *design abaci*. No further optimisation constraints need to be added to the problem formulation. Three main consequences immediately follow: firstly, the proposed method is completely geometry-based and does not depend upon the underlying mesh. In this sense, the definition of the minimum length scale becomes totally independent from the mesh size. Secondly, the minimum length scale can be controlled not only on the FE model of the structure but also on the reassembled geometry at the end of the optimisation process. Thirdly, it has been shown that the designer can decide to set knot vector according an *ad hoc* criterion and, consequently, to perform TO with a different minimum length scale in different regions of the domain. Of course, all these aspects can be controlled by properly tuning the NURBS parameters.

Two evident perspectives can be identified.

Firstly, the derived abaci can be used, in a conservative sense, in the framework of NURBS entities but their utilisation is rigorously justified only in the case of B-Spline entities. Indeed, for NURBS entities, the current

formulation of the minimum length scale could be considered valuable only from a practical viewpoint, as it provides a sort of rule of thumb for forecasting the minimum member size in TO problems. In this background, closed-form solution for Greville’s abscissae for NURBS entities must be derived and integrated within the algorithm proposed in this work in order to obtain pertinent abaci.

Secondly, some promising results can be obtained by varying the knot vector components in the NURBS-based SIMP method for TO. In particular, *ad hoc* knot vector distributions could be proposed to accomplish extremely specific tasks. In particular, the difference between the predicted and measured minimum member size can be minimised by acting on the non-trivial components of the knot-vectors of Eq. (6) which should not be set as uniformly distributed in the interval $]0, 1[$. Rather, these quantities should be integrated into the vector of design variables in order to reduce the difference between measured and forecast minimum scale length and to improve the quality of results by exactly meeting the constraint on the minimum length scale on the overall computation domain.

Moreover, these aspects go beyond the minimum length scale requirement. The knot vector components together with the number of control points and blending functions degree along each parametric direction could be simultaneously optimised in order to satisfy both minimum and maximum scale requirements. One could act, on the one hand, on the number of control points and degrees to smartly tune the number of knot vector components and, on the other hand, on the value of the non-trivial components of each knot vector to locally satisfy the minimum and maximum scale requirements. Research is ongoing on these aspects.

Acknowledgements

The first author is grateful to the Nouvelle-Aquitaine region for its contribution to this paper through the FUTURPROD project.

References

- [1] B. S. Lazarov, F. Wang, O. Sigmund, Length scale and manufacturability in density-based topology optimization, *Archive of Applied Mechanics* 86 (1) (2016) 189–218. doi:10.1007/s00419-015-1106-4.

- [2] M. Zhou, Y. K. Shyy, H. L. Thomas, Checkerboard and minimum member size control in topology optimization, *Structural and Multidisciplinary Optimization* 21 (2) (2001) 152–158. [doi:10.1007/s001580050179](https://doi.org/10.1007/s001580050179).
- [3] Altair Engineering Inc, HyperWorks 13.0, OptiStruct User`s Guide (2014).
- [4] M. Bendsoe, O. Sigmund, *Topology Optimization - Theory, Methods and Applications*, Springer, 2003.
- [5] T. A. Poulsen, A new scheme for imposing a minimum length scale in topology optimization, *International Journal for Numerical Methods in Engineering* 57 (6) (2003) 741–760. [doi:10.1002/nme.694](https://doi.org/10.1002/nme.694).
- [6] J. K. Guest, J. H. Prvost, T. Belytschko, Achieving minimum length scale in topology optimization using nodal design variables and projection functions, *International Journal for Numerical Methods in Engineering* 61 (2) (2004) 238–254. [doi:10.1002/nme.1064](https://doi.org/10.1002/nme.1064).
- [7] O. Sigmund, Manufacturing tolerant topology optimization, *Acta Mechanica Sinica* 25 (2) (2009) 227–239. [doi:10.1007/s10409-009-0240-z](https://doi.org/10.1007/s10409-009-0240-z).
- [8] F. Wang, B. S. Lazarov, O. Sigmund, On projection methods, convergence and robust formulations in topology optimization, *Structural and Multidisciplinary Optimization* 43 (6) (2011) 767–784. [doi:10.1007/s00158-010-0602-y](https://doi.org/10.1007/s00158-010-0602-y).
- [9] J. Sethian, *Level Set Methods and Fast Marching Methods: Evolving Interfaces in Computational Geometry, Fluid Mechanics, Computer Vision, and Materials Science*, Cambridge University Press, 1999.
- [10] G. Allaire, F. Jouve, A.-M. Toader, Structural optimization using sensitivity analysis and a level-set method, *Journal of Computational Physics* 194 (1) (2004) 363 – 393. [doi:https://doi.org/10.1016/j.jcp.2003.09.032](https://doi.org/10.1016/j.jcp.2003.09.032).
- [11] N. P. van Dijk, K. Maute, M. Langelaar, F. van Keulen, Level-set methods for structural topology optimization: a review, *Structural and Multidisciplinary Optimization* 48 (3) (2013) 437–472. [doi:10.1007/s00158-013-0912-y](https://doi.org/10.1007/s00158-013-0912-y).

- [12] X. Guo, W. Zhang, W. Zhong, Explicit feature control in structural topology optimization via level set method, *Computer Methods in Applied Mechanics and Engineering* 272 (2014) 354 – 378. doi:<https://doi.org/10.1016/j.cma.2014.01.010>.
- [13] W. Zhang, W. Zhong, X. Guo, An explicit length scale control approach in simp-based topology optimization, *Computer Methods in Applied Mechanics and Engineering* 282 (2014) 71 – 86. doi:<https://doi.org/10.1016/j.cma.2014.08.027>.
- [14] G. Michailidis, Manufacturing Constraints and Multi-Phase Shape and Topology Optimization via a Level-Set Method, Ph.D. thesis, Ecole Polytechnique X (2014).
- [15] G. Allaire, F. Jouve, G. Michailidis, Thickness control in structural optimization via a level set method, *Structural and Multidisciplinary Optimization* 53 (6) (2016) 1349–1382. doi:[10.1007/s00158-016-1453-y](https://doi.org/10.1007/s00158-016-1453-y).
- [16] M. Zhou, B. S. Lazarov, F. Wang, O. Sigmund, Minimum length scale in topology optimization by geometric constraints, *Computer Methods in Applied Mechanics and Engineering* 293 (2015) 266 – 282. doi:<https://doi.org/10.1016/j.cma.2015.05.003>.
- [17] Y. Gu, X. Qian, B-spline based robust topology optimization, in: Volume 2B: 41st Design Automation Conference, International Design Engineering Technical Conferences and Computers and Information in Engineering Conference, 2015. doi:[10.1115/DETC2015-46076](https://doi.org/10.1115/DETC2015-46076).
- [18] X. Qian, Topology optimization in B-spline space, *Computer Methods in Applied Mechanics and Engineering* 265 (2013) 15 – 35. doi:<https://doi.org/10.1016/j.cma.2013.06.001>.
- [19] G. Costa, M. Montemurro, J. Pailhès, A 2D topology optimisation algorithm in NURBS framework with geometric constraints, *International Journal of Mechanics and Materials in Design* 14 (4) (2018) 669 – 696. doi:[10.1007/s10999-017-9396-z](https://doi.org/10.1007/s10999-017-9396-z).
- [20] L. Piegl, W. Tiller, *The NURBS book*, Springer, Berlin, Heidelberg, 1997. doi:<https://doi.org/10.1007/978-3-642-97385-7>.

- [21] G. Costa, M. Montemurro, J. Pailhès, A NURBS-based Topology Optimisation method including additive manufacturing constraints, in: J. S. Gomes, S. A. Meguid (Eds.), Proceedings of the 7th International Conference on Mechanics and Materials in Design, INEGI/FEUP, Albufeira, Portugal, 2017.
- [22] G. Costa, M. Montemurro, J. Pailhès, A Geometry-based Method for 3D Topology Optimization, in: First International Conference on Mechanics of Advanced Materials and Structures - Proceedings, Turin, Italy, 2018.
- [23] G. Costa, M. Montemurro, J. Pailhès, [NURBS Hyper-surfaces for 3D Topology Optimisation Problems](#), Mechanics of Advanced Materials and Structures.
URL <https://doi.org/10.1080/15376494.2019.1582826>
- [24] M. Bendsoe, N. Kikuchi, Generating optimal topologies in structural design using a homogenization method, Computer Methods in Applied Mechanics and Engineering 71 (1988) 197–224.
- [25] M. Wang, X. Qian, Efficient Filtering in Topology Optimization via B-Splines, ASME, Journal of Mechanical Design 137 (3) (2015) 225–251.
[doi:10.1115/1.4029373](https://doi.org/10.1115/1.4029373).
- [26] M. Montemurro, A contribution to the development of design strategies for the optimisation of lightweight structures, HDR Thesis, Université de Bordeaux, France, 2018.
- [27] G. Farin, Curves and Surfaces for CAGD: A Practical Guide, 5th Edition, Morgan Kaufmann Publishers Inc., San Francisco, CA, USA, 2002.